Supplemental Figure 1

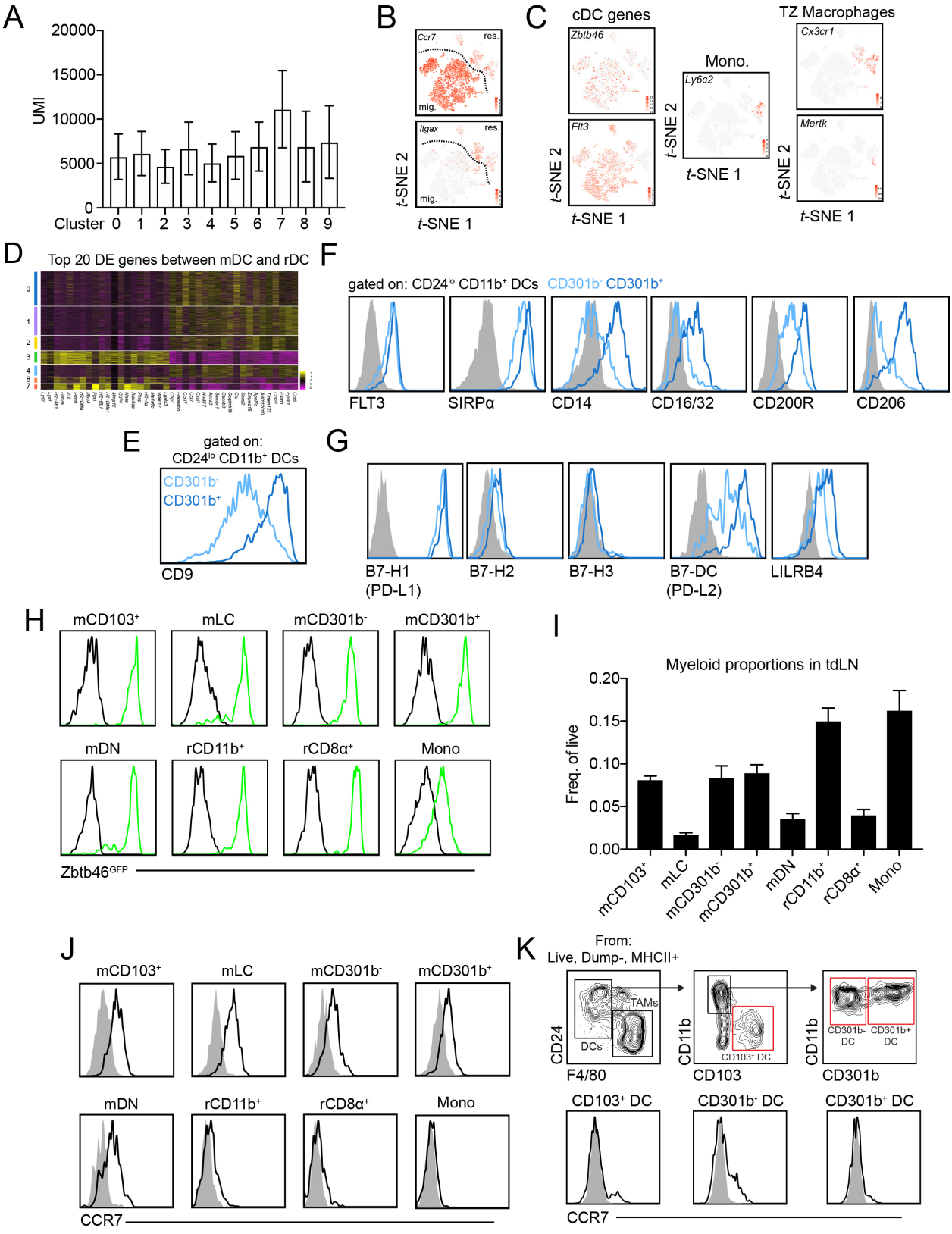

Supplemental Figure 1 Unbiased scRNA-seq of myeloid cells in the tdLN reveals extensive heterogeneity, **relates to Figure 1**
(A) Average cell UMI across the 10 clusters present in the tdLN *t*-SNE (Figure 1A) with bars denoting standard deviation. **(B)** Gene expression overlay of *Ccr7* and *Itgax* plotted on the tdLN *t*-SNE. Scale bar indicates relative expression level. **(C)** Gene expression overlay of canonical cDC markers, *Zbtb46* and *Flt3* on the tdLN *t*-SNE (left), monocyte marker *Ly6c2* (middle) and T cell zone macrophage markers *Cx3cr1* and *Mertk* (right)**.** **(D)** Heatmap displaying top 20 DE genes for mDC and rDC when clusters 0, 1, 2, 4 and 6 are compared to clusters 3 and 7 (ranked by log N fold change). **(E)** Surface expression of CD9 on $CD301b^-$ and $CD301b^+$ $CD11b^+$ $CD24^{lo}$ DC populations. **(F)** Surface expression of denoted cell markers on $mCD301b^-$ and $mCD301b^+$. (**G**) Surface expression of known inhibitory receptors on $mCD301b^-$ and $mCD301b^+$. (**H**) GFP expression in myeloid populations detected in tdLNs from tumor-bearing $Zbtb46^{GFP}$ (green) and control (black) mice. (**I**) Frequency of myeloid populations within the tdLN. **(J)** Surface levels of CCR7 on tdLN myeloid populations. **(K)** Gating strategy of myeloid populations in mouse TME (**top**) and surface expression of CCR7 on tumor DC populations (**bottom**).

Supplemental Figure 2

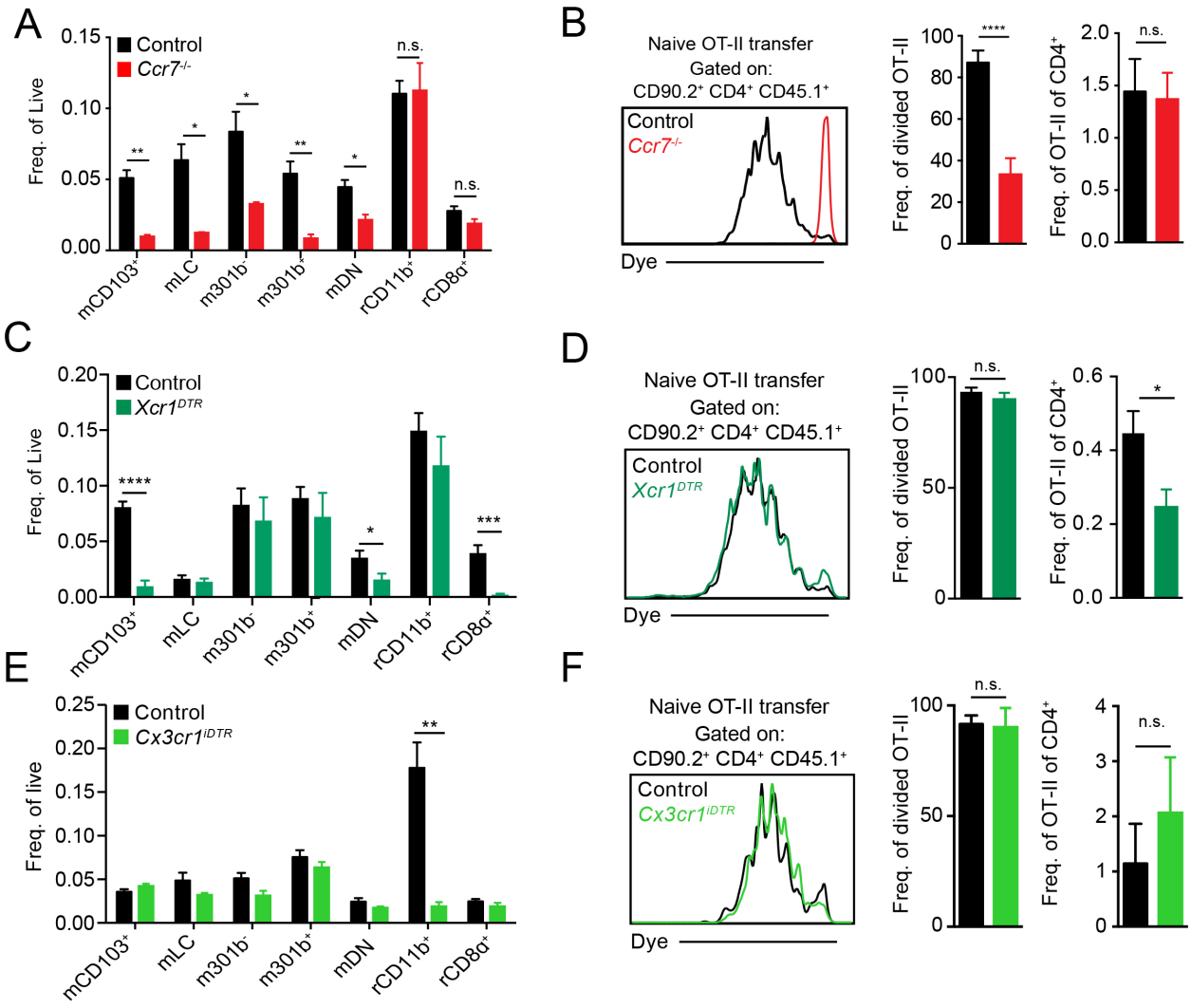

Supplemental Figure 2 mCD301b$^{-/+}$ cDC2 are uniquely able to induce anti-tumor CD4^{+} T_{conv} proliferation but fail to initiate CD4^{+} T_{conv} differentiation, **relates to Figure 2**
(A) Frequency of tdLN DC populations in control or *Ccr7-/-* tumor-bearing mice. **(B)** Proliferation of CD45.1^{+} CD4^{+} OT-II T cells in tdLN that had been transferred to control or *Ccr7-/-* tumor-bearing mice 3 days prior as assessed by dye dilution (**left**), the frequency that had divided (**middle**), and their frequency of endogenous CD4^{+} T cells (**right**). **(C)** Frequency of tdLN DC populations in control or *Xcr1^{DTR}* tumor-bearing mice. **(D)** Proliferation of transferred CD45.1^{+} CD4^{+} OT-II T cells in tdLN of DT-treated control or *Xcr1^{DTR}* tumor-bearing mice with analysis of dye dilution (**left**), the frequency that had divided (**middle**), and their frequency of endogenous CD4^{+} T cells (**right**) 3 days post-transfer. **(E)** Frequency of tdLN DC populations in DT-treated control or *Cx3cr1^{iDTR}* tumor-bearing mice. **(F)** Proliferation of transferred CD45.1^{+} CD4^{+} OT-II T cells in tdLN of DT-treated control or *Cx3cr1^{iDTR}* tumor-bearing mice with analysis of dye dilution (**left**), the frequency that had divided (**middle**), and their frequency of endogenous CD4^{+} T cells (**right**) 3 days post-transfer. Data are represented as average ± SEM unless explicitly specified. *P <0.05, **P<0.01, ***P<0.001, ****P<0.0001.

Supplemental Figure 3

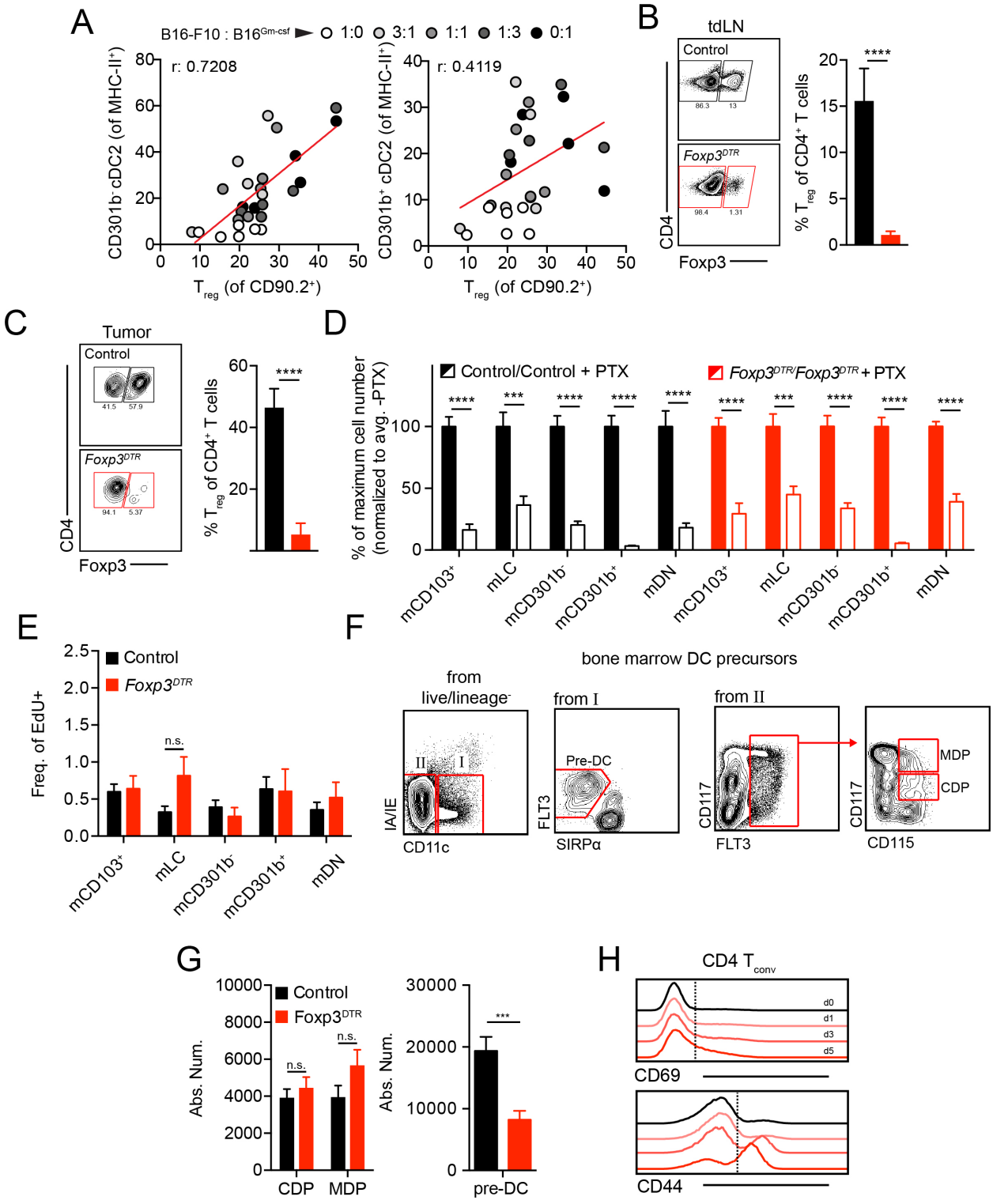

Supplemental Figure 3 Regulatory T cell depletion enhances cDC2 migration to the tdLN and unleashes an anti-tumor $CD4^+$ T_{conv} response, **related to Figure 3.**
(A) Dot plot correlation of intratumoral $CD11b^+$ $CD301b^-$ cDC2 frequency within MHC-II^+ cells (**left**) or $CD11b^+$ $CD301b^-$ cDC2 within MHC-II^+ (**right**) and T_{reg} frequency within $CD90.2^+$ T cells. Best fit line shown. Pearson correlation performed for r value. Data pooled from two experiments. **(B,C)** Gating example of FoxP3 expression in $CD4^+$ T cells of DT-treated control and *Foxp3^{DTR}* mice and the frequency of $FoxP3^+$ T_{reg} within $CD4^+$ T cells in the (**B**) tdLN or (**C**) tumor. (**D**) Control and *Foxp3^{DTR}* B16-F10 tumor-bearing mice were treated with DT and PTX and absolute number of migratory DC in the tdLN were analyzed at day 5 post-DT. Samples normalized to their genetic -PTX condition. Representative data of two independent experiments displayed. (**E**) Frequency of EdU incorporation after 2 hours within migratory DC from tumor-bearing control and *Foxp3^{DTR}* mice 2 days post-DT administration. (**F**) Representative gating scheme for DC precursors in mouse bone marrow. (**G**) Absolute numbers of DC precursors in bone marrow of tumor-bearing control and Foxp3DTR animals 5 days after DT administration. (**H**) Representative histograms of CD69 and CD44 surface levels from data in Figure 3H. Data are represented as ± SEM. *P <0.05, **P<0.01, ***P<0.001, ****P<0.0001.

Supplemental Figure 4

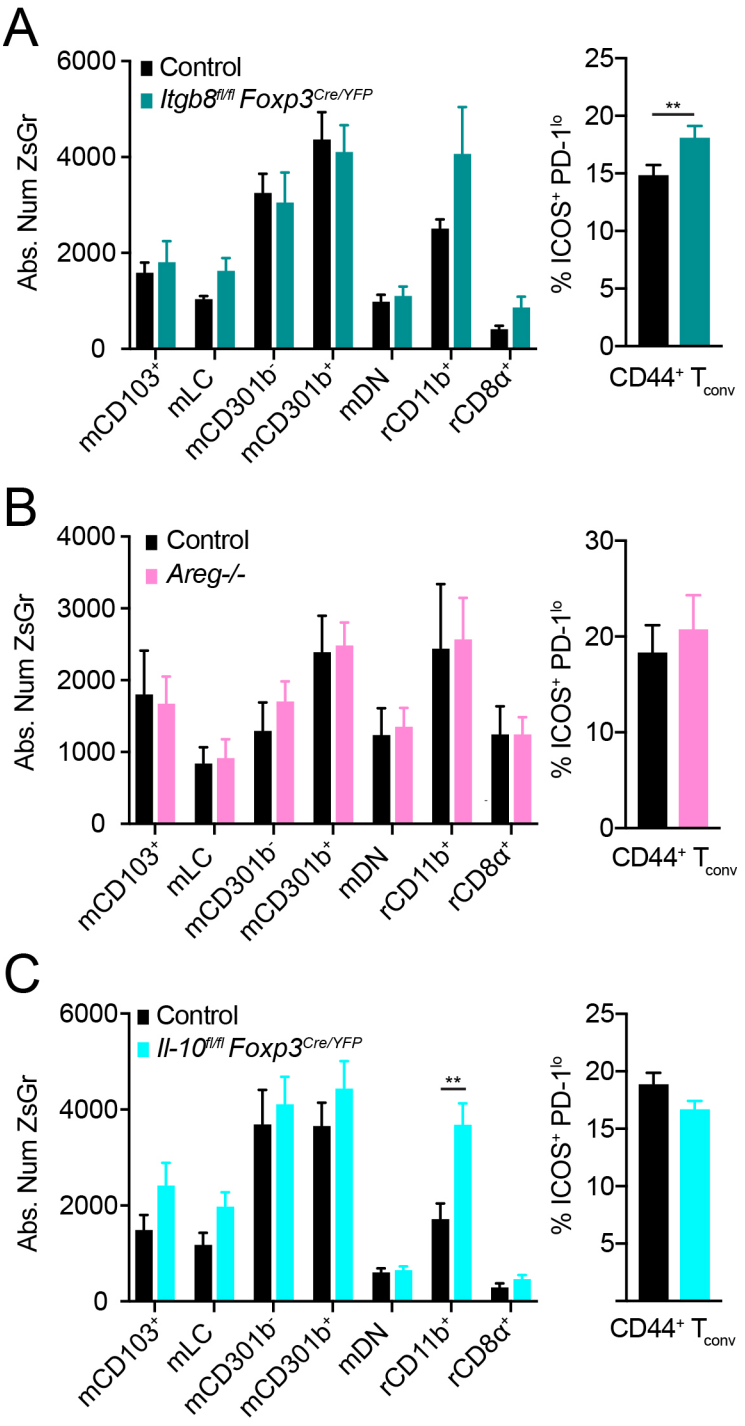

Supplementary Figure 4 Regulatory T cell depletion enhances cDC2 function and $CD4^+$ T_{conv} differentiation, **related to Figure 3 and Figure 4.**
(A) Analysis of immune populations in tdLN from $B16^{ZsGreen}$ tumor-bearing control and *Itgb8*$^{fl/fl}$*Foxp3*^{CreYFP} mice. Absolute number of $ZsGreen^+$ DC populations (left) and frequency of $CD44^+$ $CD4^+$ T_{conv} with $ICOS^+$ PD-1^{lo} surface phenotype (right). **(B)** Analysis of immune populations in tdLN from $B16^{ZsGreen}$ tumor-bearing control and *Areg-/-* mice. Absolute number of $ZsGreen^+$ DC populations (left) and frequency of $CD44^+$ $CD4^+$ T_{conv} with $ICOS^+$ PD-1^{lo} surface phenotype (right). **(C)** Analysis of immune populations in tdLN from $B16^{ZsGreen}$ tumor-bearing control and *Il-10*$^{fl/fl}$*Foxp3*^{CreYFP} mice. Absolute number of $ZsGreen^+$ DC populations (left) and frequency of $CD44^+$ $CD4^+$ T_{conv} with $ICOS^+$ PD-1^{lo} surface phenotype (right).
Supplemental Figure 4

Supplemental Figure 5

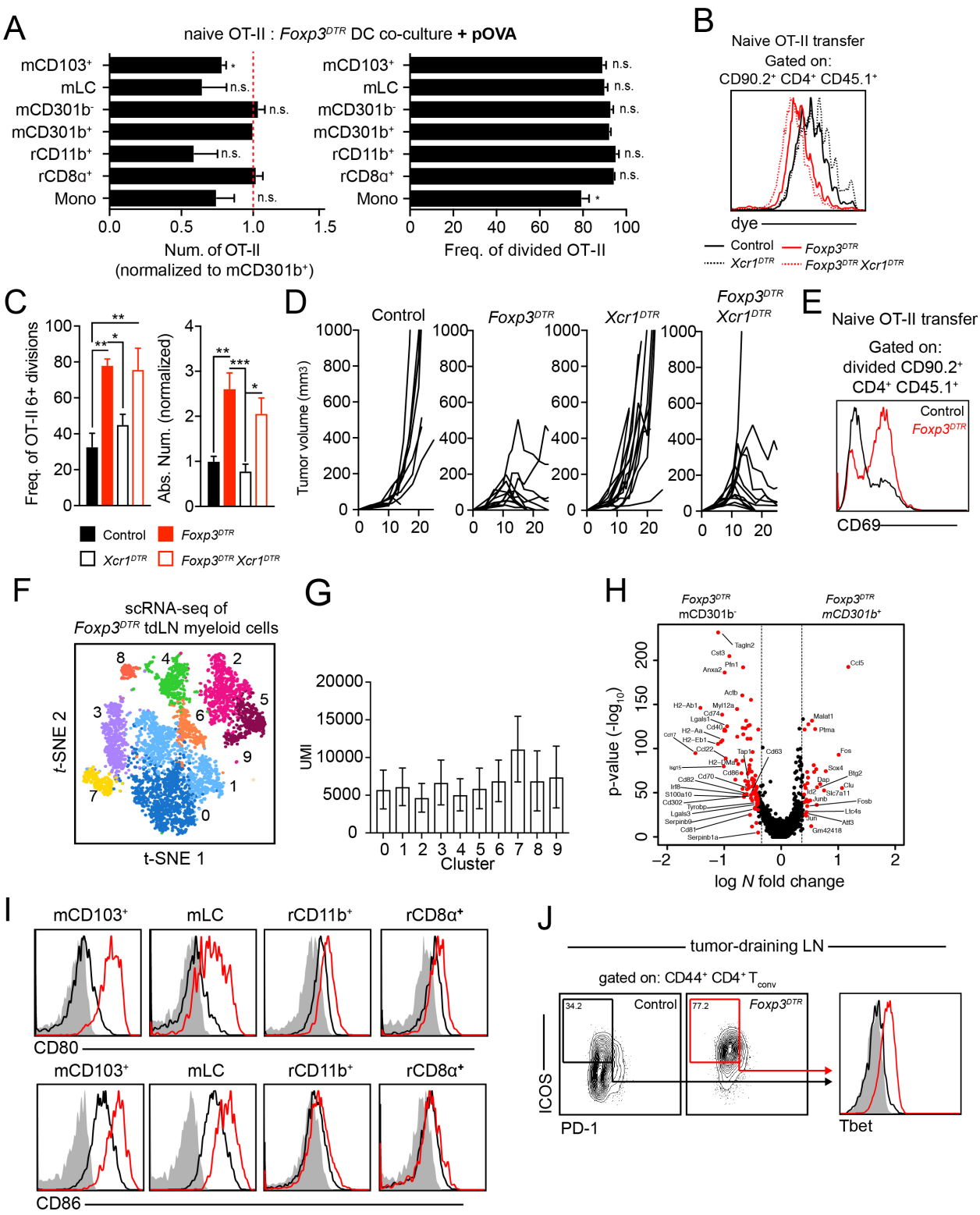

Supplementary Figure 5 Regulatory T cell depletion enhances cDC2 function and $CD4^+$ T_{conv} differentiation, **related to Figure 4.**
(A) OT-II T cells were co-cultured with APC populations sorted from DT-treated *Foxp3^{DTR}* tdLN in media containing exogenous OVA peptide (323-339) and analyzed 3 days later for the absolute number of live (**left**) OT-II T cells recovered and the frequency of cells that had divided (**right**). Data was normalized and statistically compared to $mCD301b^+$ condition. (**B**) Proliferation of $CD45.1^+$ $CD4^+$ OT-II T cells in tdLN that had been transferred to control, *Foxp3^{DTR}*, *Xcr1^{DTR}*, or *Foxp3^{DTR}Xcr1^{DTR}* tumor-bearing mice 3 days prior as assessed by dye dilution (**left**). Frequency of OT-II that divided 6+ times (**middle**). The absolute number of transferred OT-II (**right**). (**C**) Tumor growth from control, *Foxp3^{DTR}, Xcr1^{DTR} and Foxp3^{DTR}Xcr1^{DTR}* mice. Results depict tumor growth curves of individual mice. **(D)** Cell surface CD69 levels on divided OT-II T cells 3 days after transfer into DT-treated control and *Foxp3^{DTR}* $B16^{ChOVA}$ tumor-bearing mice. Representative data of three independent experiments displayed. **(E)** *t*-SNE plot and graph-based clustering of $CD90.2^-$ $B220^-$ $NK1.1^-$ $CD11b^+$ and/or $CD11c^+$ myeloid cells sorted from a DT-treated *Foxp3^{DTR}* B16F10 tdLN and processed for scRNA-seq. Each dot represents a single cell. **(F)** Average cell UMI across the 10 clusters present in the primary *Foxp3^{DTR}* tdLN *t*-SNE from Supplemental **Figure 6E** with bars denoting standard deviation. **(G)** *t*-SNE display and graph-based clustering of aggregated control and Foxp3DTR tdLN sequenced cells (**left**). Cellular origin within the aggregated *t*-SNE highlighted (**middle, right**). (**H**) Volcano plots displaying DE expressed genes comparing Foxp3DTR tdLN $mCD301b^-$ and $mCD301b^+$. Log *N* fold cutoff of 0.4 used. Genes of interest labelled. (**I**) Cell surface levels of CD80 (**left**) and CD86 (**right**) on $mCD103^+$, mLC, $rCD11b^+$ and $mCD8\alpha^+$ in control and *Foxp3^{DTR}* tdLN.

Supplemental Figure 6

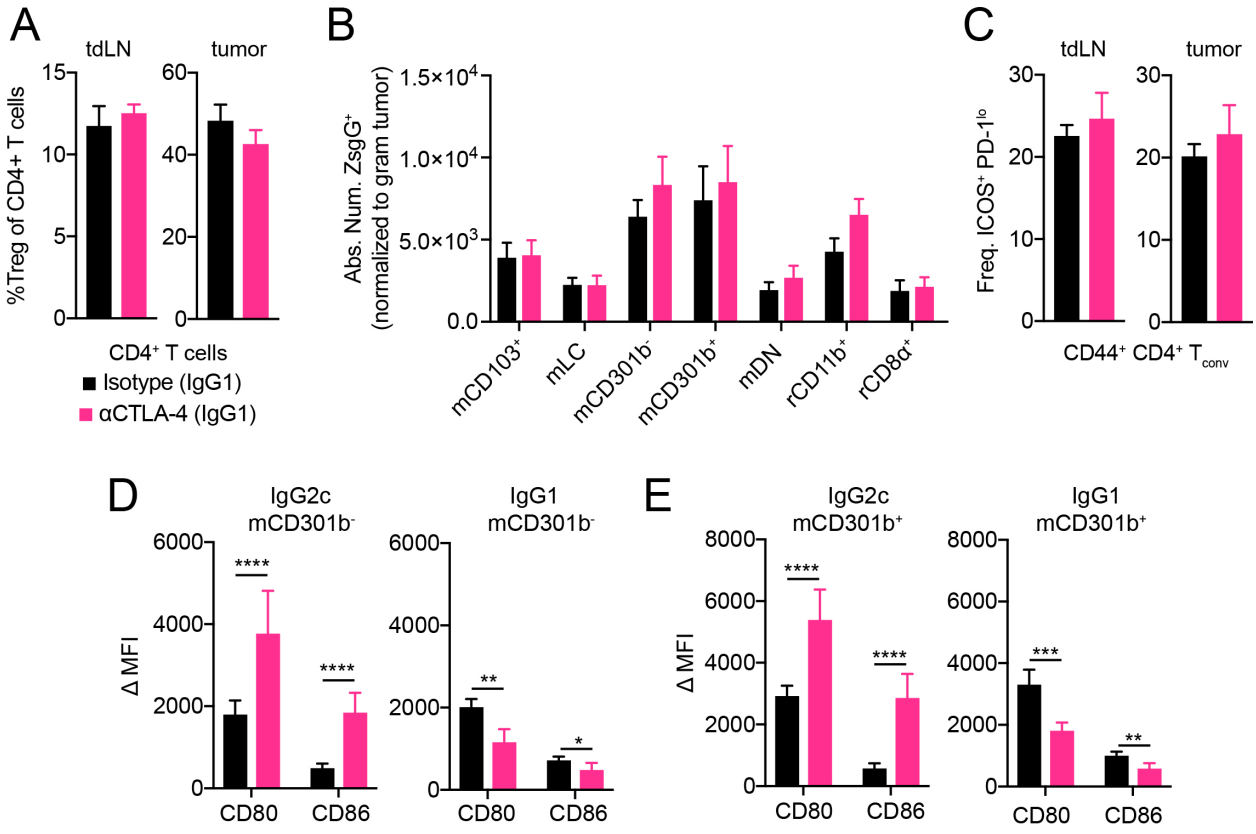

Supplemental Figure 6 Anti-CTLA-4 induces expansion and functional enhancement of CD11b^{+} cDC2, **related to Figure 5**
(**A**) Frequency of T_{reg} within CD4^{+} T cells in tdLN (left) or tumor (right) from B16^{ZsGreen} tumor-bearing mice treated with mouse IgG1 isotype or anti-CTLA-4 with a mouse IgG1 Fc. (**B**) Absolute number of ZsGreen^{+} DC in tdLN (normalized to weight of associated tumor). (**C**) Frequency of CD44^{+} CD4^{+} T_{conv} with ICOS^{+} PD-1^{lo} surface phenotype in tdLN (left) or tumor (right). (**D**) ∆MFI (CD80/CD86 MFI – Isotype MFI) from mCD301b^{-} from tdLN of B16^{ZsGreen} tumor-bearing mice treated with either Isotype/anti-CTLA-4 IgG2c (left) or Isotype/anti-CTLA-4 IgG1 (right). (**E**) ∆MFI (CD80/CD86 MFI – Isotype MFI) from mCD301b^{+} from tdLN of B16^{ZsGreen} tumor-bearing mice treated with either Isotype/anti-CTLA-4 IgG2c (left) or Isotype/anti-CTLA-4 IgG1 (right).

Supplemental Figure 7

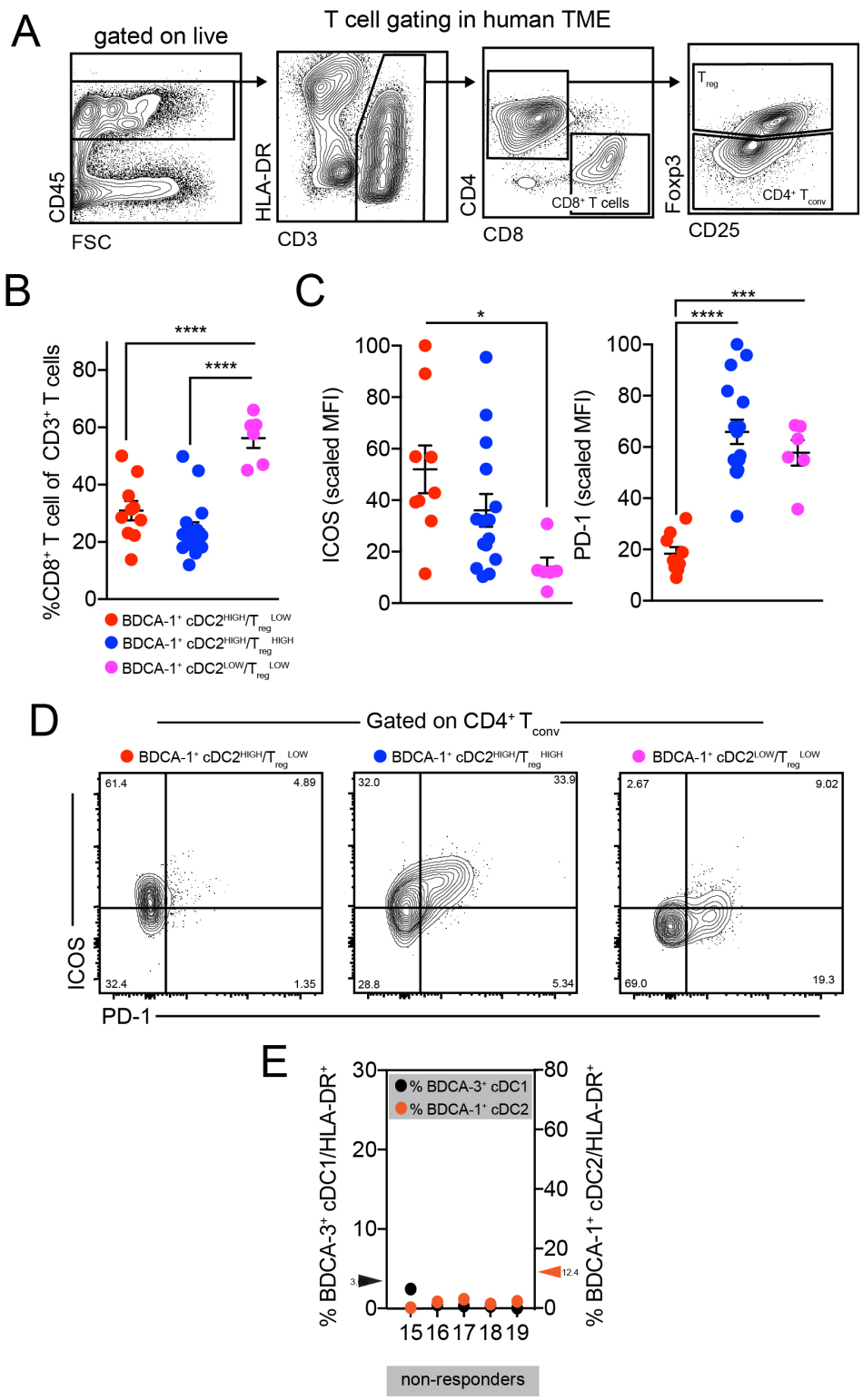

Supplementary Figure 7 BDCA-1$^+$ cDC2 proportion in the human TME impacts CD4$^+$ T_{conv} proportion and quality, **related to Figure 7**
(**A**) Gating strategy of human HNSC TME to identify T cell populations. (**B**) Frequency of CD8$^+$ T cells (of CD3$^+$ T cells) within each type of HNSC TME identified in Figure 7A. (**C**) Scaled ICOS (**left**) and PD-1 (**right**) MFI on CD4$^+$ T_{conv} within each type of HNSC TME identified in Figure 7A (**left**). (**D**) Representative example of ICOS and PD-1 expression on CD4$^+$ T_{conv} within each HNSC TME subset. (**E**) Frequency of BDCA-3$^+$ cDC1 (black) and BDCA-1+ cDC2 (orange) within HLA-DR$^+$ cells in human melanoma tumors from 5 anti-PD-1 non-responders.

Supplement Table 1

A)

ImmGen population	sample name	replicates
DC.8+.SLN	Resident CD8a+ DC(rCD8a+)	3
DC.4+.SLN	Resident CD11b+ DC (rCD11b+)	3
DC.IIhilang-103-11blo.SLN	Migratory CD11b- CD103- DC (mDN)	3
DC.IIhilang+103+11blo.SLN	Migratory (CD103+ DC) mCD103+	3
DC.IIhilang+103-11b+.SLN	Langerhans Cell (mLC)	3
DC.IIhilang-103-11b+.SLN	Migratory CD11b+ DC (mCD11b+)	3
Mo.6C+II-.Bl	Monocytes (Mono)	5
Mo.6C+II+.Bl		

B)

	Gene	logFC	AveExpr	adj.P.Val	population
	Clec9a	6.0453	5.8463	2.3E-07	rCD8a+
*	Xcr1	5.2157	6.4971	3.4E-14	rCD8a+
*	Gcsam	4.5376	5.8064	2.3E-11	rCD8a+
	Cxcl9	4.4250	7.2124	2.3E-07	rCD8a+
*	Hepacam2	4.4128	5.5057	9.8E-11	rCD8a+
*	Tlr3	4.2569	5.7582	6.8E-14	rCD8a+
*	Snx22	3.1860	6.3865	7.8E-11	rCD8a+
*	Pdia5	3.1521	7.0875	1.8E-11	rCD8a+
*	Clnk	3.0847	5.8176	9.6E-13	rCD8a+
	Fam149a	2.7531	6.3720	1.8E-10	rCD8a+
*	Clec1a	2.7458	5.2666	4.2E-11	rCD8a+
*	Cxcr3	2.7181	7.3807	9.4E-12	rCD8a+
*	1700009J07Rik	2.6434	5.8070	9.4E-12	rCD8a+
	Itgae	2.4314	5.9630	1.3E-07	rCD8a+
	Notch4	2.1416	6.8418	6.2E-10	rCD8a+
	Dbn1	2.1235	6.8576	1.1E-08	rCD8a+
	Naga	1.8590	9.9249	9.2E-08	rCD8a+
	Ifnlr1	1.6591	6.2720	2.7E-07	rCD8a+
	Eefsec	1.6021	7.9756	1.1E-08	rCD8a+
	Arid3b	1.4773	6.9577	1.2E-07	rCD8a+
*	Mmp12	4.8078	6.0647	3.4E-13	rCD11b+
*	Mgl2	4.6375	5.7625	1.7E-08	rCD11b+
*	Cd4	3.6664	6.5537	6.1E-09	rCD11b+
	Rgl1	2.8025	6.9580	9.6E-06	rCD11b+
*	Klrb1b	2.6520	5.6951	5.2E-07	rCD11b+
	Egr2	2.6413	6.8819	6.3E-07	rCD11b+
*	Hr	2.2537	6.6558	9.2E-10	rCD11b+
	Cd209d	2.0825	5.3407	1.4E-04	rCD11b+
	Lphn3	1.8031	4.6999	8.3E-07	rCD11b+
*	Fcrls	1.5823	4.7863	5.0E-08	rCD11b+

	Gene	logFC	AveExpr	adj.P.Val	population
	Slc2a3	1.4923	6.7267	2.9E-04	rCD11b+
	Ctnnd2	1.4801	6.6717	1.5E-05	rCD11b+
*	Clec4g	1.4722	5.5170	3.0E-06	rCD11b+
	Cyp4f37	1.1100	4.9626	2.1E-04	rCD11b+
*	Ggt5	1.0227	6.4149	4.2E-06	rCD11b+
	Dcstamp	0.9725	5.2880	1.4E-04	rCD11b+
	Cox6b2	0.8364	6.3361	2.2E-04	rCD11b+
	Stk25	-0.8156	8.4029	3.9E-04	rCD11b+
	Arid2	-0.9218	8.8855	1.9E-04	rCD11b+
	Ermard	-1.0918	8.0013	4.6E-04	rCD11b+
*	Khdc1a	2.8835	3.9299	5.8E-07	mDN
*	Khdc1c	2.8771	5.9704	5.8E-07	mDN
*	Sned1	2.3779	7.3490	3.2E-04	mDN
*	Clmn	2.1187	5.4687	2.6E-04	mDN
	Khdc1b	1.8016	5.5040	6.0E-06	mDN
*	Gdpd1	1.3379	5.1630	2.2E-04	mDN
*	Efna5	1.3041	6.1494	2.8E-04	mDN
*	Gm15698	3.5437	5.8649	9.7E-06	mCD103+
*	Vmn2r90	3.0364	5.1163	2.5E-05	mCD103+
*	Slc27a3	2.7056	6.7149	3.6E-05	mCD103+
	Gltpd1	2.5726	7.4650	1.5E-04	mCD103+
	Arg2	2.3732	6.1897	1.7E-04	mCD103+
	Zdhhc14	2.1802	7.4723	3.2E-04	mCD103+
*	Arhgap8	1.9746	6.1339	2.4E-07	mCD103+
	Cd96	1.5481	5.2300	1.4E-04	mCD103+
*	Exoc3l4	1.5155	7.0362	1.1E-05	mCD103+
	Colq	1.3886	6.8375	3.2E-04	mCD103+
*	Mfsd4	1.3693	6.8100	2.5E-05	mCD103+
	2210409E12Rik	1.3382	6.6145	1.4E-04	mCD103+
	Erich5	1.3100	6.3656	1.1E-04	mCD103+
*	Slc18a1	1.2558	5.6380	8.9E-06	mCD103+
	Sprr4	1.0699	5.9662	1.5E-04	mCD103+
*	Sh3gl1	0.9942	8.6567	4.0E-05	mCD103+
	Adrm1	0.6508	8.8218	1.4E-04	mCD103+
	Adrm1	0.6500	8.7883	1.9E-04	mCD103+
*	1810011O10Rik	5.7479	4.8945	9.5E-16	mLC
*	Fam189a2	4.4585	6.1501	4.6E-11	mLC
	Fam115c	4.0949	5.7914	3.6E-12	mLC
	Npy1r	4.0426	5.4201	2.2E-07	mLC
	Atf7ip2	3.4395	5.1965	2.1E-06	mLC
*	Nbea	3.3415	5.3563	3.7E-12	mLC
*	Fam160a1	3.0305	6.3350	8.2E-11	mLC
	Tjp1	2.6631	5.3330	3.6E-10	mLC
*	Pcdh7	2.3367	5.5365	2.0E-08	mLC
	Pxdn	2.0861	5.8142	5.7E-08	mLC
	9330155M09Rik	2.0174	3.4478	2.0E-08	mLC
	Epb4.1l3	1.9747	5.6021	6.4E-07	mLC
	Map2	1.9451	5.4537	1.2E-07	mLC
	Fblim1	1.9175	6.1430	3.9E-07	mLC
	Apbb2	1.8244	6.4300	5.7E-07	mLC
*	Stxbp5l	1.6258	4.3168	2.4E-11	mLC
	Cadm2	1.5911	5.0181	3.9E-07	mLC

	Gene	logFC	AveExpr	adj.P.Val	population
	Tmem45b	1.4376	5.5234	2.5E-06	mLC
	Agmo	1.3380	4.1082	2.5E-06	mLC
	Aldh1a2	4.7680	6.3960	1.3E-03	mCD11b+
	Gm5486	3.8271	5.5478	9.5E-04	mCD11b+
	Serpinb9b	3.1731	6.4721	9.5E-04	mCD11b+
	Cxcl13	3.0526	5.8987	3.0E-04	mCD11b+
*	Htra1	2.8685	5.7485	7.6E-05	mCD11b+
	Rai14	2.2526	6.4865	4.6E-04	mCD11b+
*	Car2	2.1700	6.1995	8.0E-05	mCD11b+
*	Sod3	2.1562	5.5361	1.8E-05	mCD11b+
*	Grpr	2.0489	5.1700	9.6E-06	mCD11b+
*	AA467197	1.9255	5.6350	6.3E-05	mCD11b+
	Mucl1	1.8875	3.7911	2.1E-05	mCD11b+
	Depdc7	1.8215	6.1404	9.3E-04	mCD11b+
	Gm5622	1.7573	4.6778	8.1E-04	mCD11b+
	LOC102634703	1.7203	4.7592	4.3E-05	mCD11b+
	LOC101055806	1.6901	3.4570	1.8E-05	mCD11b+
	Gm10375	1.6646	3.9046	1.8E-05	mCD11b+
	LOC102634703	1.5880	4.6571	9.4E-05	mCD11b+
	Ms4a14	1.3324	3.9208	8.0E-04	mCD11b+
	Fabp4	1.2515	4.7717	4.6E-04	mCD11b+
	Gm10375	1.0393	3.8883	4.2E-04	mCD11b+
*	F13a1	7.0452	7.1382	1.4E-19	Mono
	Klra2	6.5515	5.4958	1.9E-13	Mono
	Chil3	6.0381	5.3666	1.6E-13	Mono
*	Serpinb10	5.9713	5.1624	3.2E-16	Mono
	Ms4a6d	5.5989	6.6334	2.6E-13	Mono
	Msr1	5.4280	5.4302	1.9E-13	Mono
*	Cd93	5.0419	6.4879	1.4E-19	Mono
*	Fcgr1	4.8002	7.2360	2.2E-18	Mono
*	Fgd4	4.4340	5.8459	8.1E-14	Mono
*	Arhgef37	4.2467	5.7495	1.6E-14	Mono
*	Thbd	3.6346	6.7092	3.4E-14	Mono
	Pde7b	3.3830	5.7471	8.3E-14	Mono
*	Rasgrp2	3.1460	6.7385	6.9E-15	Mono
	Oas3	2.8684	7.1183	1.7E-13	Mono
	C5ar1	2.8614	5.6460	1.8E-13	Mono
	Hip1	2.6104	6.9733	2.3E-13	Mono
	Siglec1	2.2416	6.8664	1.1E-13	Mono
	Nedd4	-4.2161	8.8719	1.8E-13	Mono
	Adam23	-6.4232	10.0104	7.1E-18	Mono

Supplemental Table 1 – related to Figure 1. ImmGen population specific gene signatures.
(**A**) ImmGen sample ID, abbreviated sample name and replicates used in creation on ImmGen population specific gene signature. (**B**) DE was performed comparing one population to the aggregate of the 6 remaining populations. DE is ranked based on log fold change. An asterisk indicates gene was detected in scRNA-seq and thus used for gene signature overlay. See materials and methods for specific process through which DE signature was generated.

Supplemental Table 2

gene	avg_logFC	pct.1	pct.2	p_val	p_val_adj	cluster
Ccl17	1.5851	0.584	0.198	5.10E-148	7.40E-144	0
Clu	1.2221	0.641	0.305	2.20E-119	3.30E-115	0
Fxyd2	1.0765	0.548	0.221	2.60E-114	3.80E-110	0
Cxcl1	0.9985	0.407	0.238	8.60E-37	1.30E-32	0
Slc7a11	0.932	0.566	0.186	2.20E-136	3.20E-132	0
Fabp5	0.8807	0.959	0.628	4.20E-205	6.10E-201	0
S100a10	0.7559	0.587	0.297	2.20E-89	3.20E-85	0
Ltc4s	0.7358	0.689	0.329	8.20E-117	1.20E-112	0
Nrp2	0.723	0.534	0.183	2.00E-124	2.80E-120	0
Cstb	0.7211	0.904	0.757	9.10E-122	1.30E-117	0
Ccl5	1.3933	0.999	0.979	2.10E-226	3.10E-222	1
Epsti1	1.3074	0.995	0.885	2.00E-269	2.90E-265	1
Tnfrsf4	1.1602	0.797	0.335	5.10E-192	7.40E-188	1
Txndc17	1.1027	0.947	0.745	1.40E-227	2.00E-223	1
Zmynd15	1.045	0.947	0.537	1.20E-227	1.80E-223	1
Serpinb1a	0.9627	0.574	0.279	2.40E-74	3.50E-70	1
Laptm4b	0.9457	0.614	0.105	5.00E-259	7.20E-255	1
AW112010	0.9084	0.99	0.859	2.00E-173	3.00E-169	1
Il12b	0.8985	0.386	0.118	2.80E-82	4.00E-78	1
Mthfd2	0.8587	0.825	0.509	1.50E-148	2.20E-144	1
H2-M2	1.4223	0.998	0.55	2.10E-204	3.00E-200	2
Mfge8	1.2891	0.826	0.356	7.10E-132	1.00E-127	2
Apol7c	0.9388	0.96	0.674	6.30E-98	9.10E-94	2
1810011O10Rik	0.8978	0.317	0.007	7.90E-216	1.20E-211	2
Rgs1	0.7823	0.966	0.875	2.00E-66	3.00E-62	2
Malat1	0.7443	1	0.999	6.60E-155	9.60E-151	2
Tsc22d3	0.695	0.593	0.343	2.00E-45	2.90E-41	2
Fscn1	0.6631	0.996	0.855	4.60E-75	6.70E-71	2
Ccl22	0.6486	0.87	0.607	1.70E-51	2.50E-47	2
Ankrd33b	0.6299	0.847	0.564	7.50E-57	1.10E-52	2
Lyz1	2.0233	0.312	0.114	4.30E-31	6.20E-27	3
Mmp12	1.8648	0.374	0.011	1.50E-238	2.20E-234	3
H2-DMb2	1.5699	0.89	0.234	2.60E-224	3.90E-220	3
Il1b	1.538	0.851	0.282	1.30E-156	1.90E-152	3
H2-Ab1	1.522	1	0.863	1.20E-170	1.70E-166	3
Gm2a	1.5003	0.94	0.289	2.60E-219	3.80E-215	3
Cd209a	1.4702	0.333	0.022	1.50E-158	2.20E-154	3
H2-DMa	1.3199	0.976	0.434	1.90E-177	2.80E-173	3
H2-Eb1	1.2644	1	0.889	7.10E-159	1.00E-154	3
Cd74	1.2485	1	0.995	1.40E-174	2.00E-170	3
Cd1d1	1.2515	0.608	0.133	1.20E-142	1.80E-138	4
Glipr2	1.1335	0.873	0.438	1.50E-116	2.20E-112	4
Rnaset2a	1.102	0.654	0.346	1.30E-62	1.90E-58	4
Phf11b	0.9192	0.804	0.417	2.90E-91	4.20E-87	4
Gnl2	0.8176	0.728	0.408	2.80E-59	4.00E-55	4
Tubb5	0.8088	0.99	0.862	1.10E-98	1.50E-94	4
Socs2	0.7804	0.972	0.668	3.60E-87	5.30E-83	4
Isg15	0.7668	0.565	0.261	9.60E-46	1.40E-41	4
Cnn2	0.7533	0.919	0.692	1.30E-74	1.80E-70	4
Fabp5	0.7444	0.954	0.693	1.30E-65	1.90E-61	4

gene	avg_logFC	pct.1	pct.2	p_val	p_val_adj	cluster
Apoe	3.2821	0.599	0.174	8.40E-121	1.20E-116	5
Lyz2	3.0937	0.987	0.488	4.20E-228	6.20E-224	5
C1qb	2.7224	0.398	0.043	4.00E-151	5.90E-147	5
Plac8	2.6962	0.804	0.168	4.90E-222	7.20E-218	5
C1qa	2.6874	0.357	0.044	1.80E-122	2.60E-118	5
Ly6i	2.5799	0.829	0.041	0.00E+00	0.00E+00	5
Ifi27l2a	2.3491	0.895	0.234	4.90E-241	7.10E-237	5
Ifitm3	2.274	0.934	0.257	2.50E-238	3.70E-234	5
C1qc	2.2405	0.36	0.025	4.00E-170	5.90E-166	5
Ms4a6c	2.0391	0.98	0.163	0.00E+00	0.00E+00	5
Cd209d	1.6266	0.276	0.022	1.50E-83	2.20E-79	6
H2-DMb2	1.5878	0.88	0.273	5.70E-100	8.30E-96	6
Cd7	1.4582	0.411	0.036	3.40E-116	5.00E-112	6
Klrd1	1.3021	0.448	0.093	1.10E-59	1.60E-55	6
Lgals1	1.1425	0.724	0.534	6.20E-18	9.00E-14	6
Cd8a	1.0849	0.453	0.081	5.80E-65	8.40E-61	6
Atp1b1	1.0457	0.333	0.014	2.40E-150	3.50E-146	6
Gpr183	1.0352	0.771	0.22	1.20E-78	1.80E-74	6
Lag3	1.0148	0.458	0.071	8.50E-79	1.20E-74	6
H2-DMa	1.0089	0.932	0.468	7.80E-58	1.10E-53	6
Ppt1	2.4819	0.989	0.219	1.20E-183	1.80E-179	7
Naaa	2.2571	0.949	0.105	1.20E-260	1.70E-256	7
Xcr1	1.7113	0.876	0.01	0.00E+00	0.00E+00	7
Plbd1	1.6669	0.989	0.245	8.30E-148	1.20E-143	7
Cd8a	1.6579	0.921	0.061	0.00E+00	0.00E+00	7
Ifi205	1.5409	0.899	0.044	0.00E+00	0.00E+00	7
Ckb	1.4272	0.865	0.109	3.20E-191	4.60E-187	7
Cst3	1.4052	1	0.993	4.10E-87	6.00E-83	7
Psap	1.3847	0.994	0.888	3.10E-86	4.50E-82	7
Cxcl9	1.3386	0.747	0.074	1.10E-183	1.60E-179	7

Supplemental Table 2 – related to Figure 1. Top 10 DE genes between all myeloid clusters in mouse tdLN scRNA-Seq

DE was performed where every cluster was compared to all remaining cells. The top 10 DE genes for each cluster was selected and displayed in the Figure 1C and Supplementary Table 2. DE parameters: logfc.threshold = 0.4, min.pct = 0.25.

Supplemental Table 3

gene	avg_logFC	pct.1	pct.2	p_val	p_val_adj	up in cluster
Ccl5	2.4898	0.996	0.951	1.2E-237	1.8E-233	mig
Epsti1	2.1779	0.97	0.686	2.7E-238	3.9E-234	mig
Fscn1	2.1234	0.985	0.556	1.2E-259	1.8E-255	mig
Ccl22	1.9804	0.764	0.271	1.1E-137	1.6E-133	mig
Tmem123	1.9144	0.995	0.681	6.1E-279	8.9E-275	mig
AW112010	1.8506	0.947	0.647	1.1E-211	1.6E-207	mig
Apol7c	1.7747	0.831	0.351	4.6E-146	6.8E-142	mig
Zmynd15	1.6995	0.766	0.21	1.4E-150	2.1E-146	mig
Socs2	1.5899	0.866	0.198	3.5E-205	5.1E-201	mig
Clu	1.5691	0.475	0.161	2.0E-55	2.9E-51	mig
Serpinb6b	1.5590	0.822	0.343	1.1E-146	1.6E-142	mig
Cacnb3	1.5470	0.88	0.218	5.6E-212	8.1E-208	mig
Samsn1	1.5230	0.961	0.4	2.8E-242	4.0E-238	mig
Anxa3	1.5110	0.957	0.366	1.1E-228	1.6E-224	mig
Nudt17	1.5007	0.859	0.239	1.8E-198	2.6E-194	mig
Cxcl1	1.4360	0.344	0.106	2.7E-35	3.9E-31	mig
Ccr7	1.4348	0.975	0.576	3.5E-196	5.0E-192	mig
Ccl17	1.4054	0.381	0.074	2.9E-50	4.2E-46	mig
Gadd45b	1.3783	0.922	0.533	8.3E-184	1.2E-179	mig
Crip1	1.3775	0.997	0.923	4.7E-211	6.8E-207	mig
Lgals3	-1.3272	0.455	0.849	1.7E-136	2.4E-132	res
Wfdc17	-1.3345	0.074	0.472	1.6E-155	2.3E-151	res
Ms4a6c	-1.3710	0.06	0.703	0.0E+00	0.0E+00	res
H2-Aa	-1.4673	0.925	1	6.2E-251	9.1E-247	res
Psap	-1.5084	0.866	0.965	1.2E-174	1.8E-170	res
Alox5ap	-1.5244	0.074	0.842	0.0E+00	0.0E+00	res
Naaa	-1.5248	0.034	0.518	2.1E-266	3.0E-262	res
Cd74	-1.5565	0.995	1	1.4E-271	2.0E-267	res
Mmp12	-1.5784	0.01	0.267	1.2E-151	1.7E-147	res
H2-DMb1	-1.5802	0.247	0.911	1.4E-299	2.1E-295	res
H2-Eb1	-1.6460	0.878	1	2.0E-264	3.0E-260	res
Ppt1	-1.6539	0.146	0.595	4.9E-152	7.1E-148	res
Ifitm3	-1.7392	0.172	0.697	5.9E-192	8.6E-188	res
H2-DMa	-1.7663	0.342	0.976	0.0E+00	0.0E+00	res
Plbd1	-1.8892	0.087	0.906	0.0E+00	0.0E+00	res
Il1b	-1.8961	0.195	0.77	1.1E-218	1.6E-214	res
Gm2a	-1.9321	0.171	0.951	0.0E+00	0.0E+00	res
H2-Ab1	-2.2566	0.841	1	5.8E-295	8.5E-291	res
Lyz1	-2.4575	0.059	0.274	3.1E-62	4.5E-58	res
Lyz2	-3.2636	0.419	0.844	1.6E-157	2.3E-153	res

Supplemental Table 3 – related to Supplementary Figure 1. Top 20 DE genes between migratory and resident myeloid populations.
DE was performed where migratory clusters (0, 1, 2, 4, 6) were compared to resident clusters (3, 5, 7). The top 20 DE genes for each group was selected and displayed in Supplementary Figure 1E and Supplementary Table 3. DE parameters: logfc.threshold = 0.4, min.pct = 0.25.

Supplemental Table 4

gene	avg_logFC	pct.1	pct.2	p_val	p_val_adj	up in cluster
Clu	1.7317	0.641	0.229	1.1E-53	1.6E-49	0
Ccl17	1.6774	0.584	0.198	8.7E-42	1.3E-37	0
Cxcl1	1.3876	0.407	0.163	1.8E-21	2.7E-17	0
Fxyd2	1.1307	0.548	0.265	3.4E-30	4.9E-26	0
mt-Nd1	1.0185	0.957	0.626	4.8E-80	7.0E-76	0
mt-Cytb	0.9925	0.968	0.73	1.8E-82	2.6E-78	0
mt-Co3	0.9129	0.995	0.913	1.5E-90	2.2E-86	0
H2-M2	0.8723	0.663	0.44	5.1E-23	7.4E-19	0
Rpl36a	0.8535	0.974	0.758	2.6E-88	3.8E-84	0
mt-Nd2	0.8523	0.798	0.392	5.3E-56	7.7E-52	0
mt-Nd4	0.8232	0.923	0.598	9.7E-62	1.4E-57	0
Slc7a11	0.8232	0.566	0.232	5.8E-30	8.5E-26	0
S100a10	0.8161	0.587	0.242	1.4E-33	2.0E-29	0
mt-Atp6	0.7962	1	0.957	3.5E-78	5.0E-74	0
mt-Co2	0.7784	0.996	0.885	4.7E-77	6.8E-73	0
Ccl22	0.7737	0.8	0.578	5.0E-24	7.2E-20	0
Rps17	0.7590	0.952	0.725	5.9E-71	8.6E-67	0
Mt1	0.7568	0.657	0.379	1.4E-25	2.0E-21	0
Vim	0.7401	0.952	0.84	9.3E-40	1.4E-35	0
Cxcl2	0.7337	0.3	0.132	9.3E-12	1.4E-07	0
Adam23	0.7209	0.603	0.198	5.5E-42	8.0E-38	0
Rps8	0.7128	0.989	0.916	6.5E-81	9.5E-77	0
Ltc4s	0.7021	0.689	0.318	4.0E-38	5.9E-34	0
Rps3a1	0.6963	0.998	0.959	1.9E-102	2.8E-98	0
Cstb	0.6916	0.904	0.784	1.2E-40	1.8E-36	0
Cd9	0.6756	0.656	0.305	1.1E-34	1.6E-30	0
Serpinb1a	0.6680	0.463	0.244	1.7E-15	2.4E-11	0
Rps18	0.6561	1	0.985	3.0E-105	4.4E-101	0
Rps29	0.6548	0.999	0.969	1.6E-98	2.3E-94	0
Rpl6	0.6464	0.992	0.929	4.6E-91	6.8E-87	0
Mif4gd	-0.6031	0.316	0.603	4.7E-33	6.9E-29	4
Eno3	-0.6091	0.753	0.903	7.6E-34	1.1E-29	4
Tagln2	-0.6210	0.765	0.908	3.5E-30	5.2E-26	4
Tuba1a	-0.6211	0.868	0.957	9.5E-44	1.4E-39	4
Dok1	-0.6307	0.57	0.835	4.8E-44	6.9E-40	4
Fscn1	-0.6310	0.985	0.995	1.0E-55	1.5E-51	4
Tap2	-0.6369	0.439	0.707	2.7E-36	3.9E-32	4
Ccnd1	-0.6383	0.205	0.42	3.5E-21	5.1E-17	4
Tubb5	-0.6641	0.907	0.99	3.6E-63	5.2E-59	4
Ccnd2	-0.6779	0.065	0.321	8.3E-40	1.2E-35	4
Phf11a	-0.6810	0.162	0.483	2.0E-42	2.9E-38	4
Vwa5a	-0.6886	0.255	0.511	5.6E-31	8.2E-27	4
Rcsd1	-0.6916	0.574	0.858	1.0E-50	1.5E-46	4
Ube2l6	-0.6939	0.697	0.858	6.1E-41	8.8E-37	4
Cnn2	-0.7014	0.718	0.919	1.3E-54	1.8E-50	4
Bcl2l14	-0.7050	0.127	0.417	1.3E-39	1.9E-35	4
Psmb9	-0.7079	0.876	0.98	2.1E-80	3.1E-76	4
Epsti1	-0.7142	0.971	0.99	3.7E-63	5.4E-59	4
Rnaset2b	-0.7610	0.121	0.427	2.1E-44	3.1E-40	4
Sp140	-0.7645	0.339	0.646	5.7E-44	8.2E-40	4

gene	avg_logFC	pct.1	pct.2	p_val	p_val_adj	up in cluster
Tap1	-0.8232	0.425	0.786	2.1E-63	3.0E-59	4
Ifitm3	-0.8706	0.15	0.514	1.4E-55	2.0E-51	4
Phf11b	-0.9062	0.41	0.804	1.3E-69	1.9E-65	4
Inpp5b	-0.9081	0.134	0.557	2.0E-74	3.0E-70	4
Isg15	-0.9561	0.216	0.565	2.1E-45	3.0E-41	4
Irf8	-0.9921	0.59	0.837	1.4E-50	2.0E-46	4
Cd1d1	-1.0065	0.213	0.608	1.2E-58	1.7E-54	4
Tnfrsf4	-1.0591	0.382	0.789	4.4E-68	6.4E-64	4
Glipr2	-1.1852	0.491	0.873	8.3E-90	1.2E-85	4
Rnaset2a	-1.2969	0.25	0.654	1.4E-69	2.1E-65	4

Supplemental Table 4 – related to Figure 1. Top 30 DE genes between mCD11b$^+$ cDC2 cluster 0 and 4

DE was performed where CD11b$^+$ cDC2 cluster 0 was compared CD11b$^+$ cDC2 cluster 4. The top 30 DE genes for each group was selected and displayed in Figure 1D and Supplementary Table 4. DE parameters: logfc.threshold = 0.4, min.pct = 0.25.

Supplemental Table 5

(**A**)

gene	avg_logFC	pct.1	pct.2	p_val	p_val_adj	cluster
Ccl5	1.1778	0.999	0.996	2.55E-197	3.67E-193	mCD301b+ DTR
Clu	1.0672	0.509	0.286	4.74E-60	6.82E-56	mCD301b+ DTR
Fos	1.0095	0.759	0.498	8.32E-98	1.20E-93	mCD301b+ DTR
Sox4	0.7823	0.573	0.262	2.37E-79	3.40E-75	mCD301b+ DTR
Slc7a11	0.7527	0.562	0.353	1.84E-57	2.65E-53	mCD301b+ DTR
Dap	0.6841	0.74	0.573	1.23E-64	1.78E-60	mCD301b+ DTR
Btg2	0.6286	0.674	0.489	8.06E-61	1.16E-56	mCD301b+ DTR
Mt1	0.6236	0.681	0.477	6.46E-41	9.28E-37	mCD301b+ DTR
Zfos1	0.6148	0.836	0.69	2.17E-81	3.12E-77	mCD301b+ DTR
Ptma	0.5964	0.997	0.984	6.35E-127	9.13E-123	mCD301b+ DTR
Eif4a2	0.5777	0.87	0.746	2.15E-78	3.09E-74	mCD301b+ DTR
Npc2	0.5707	0.996	0.989	7.31E-86	1.05E-81	mCD301b+ DTR
Malat1	0.5414	1	0.998	1.13E-136	1.63E-132	mCD301b+ DTR
Gm42418	0.5265	0.666	0.693	4.30E-17	6.19E-13	mCD301b+ DTR
Pmaip1	0.5094	0.767	0.585	3.64E-46	5.24E-42	mCD301b+ DTR
Rps27	0.4762	1	0.999	1.54E-132	2.22E-128	mCD301b+ DTR
AW112010	0.4711	0.991	0.968	1.02E-71	1.46E-67	mCD301b+ DTR
Junb	0.4692	0.954	0.917	1.04E-44	1.50E-40	mCD301b+ DTR
Pnrc1	0.4622	0.862	0.791	1.17E-65	1.69E-61	mCD301b+ DTR
Fosb	0.4576	0.32	0.164	6.68E-40	9.60E-36	mCD301b+ DTR
Npm1	0.4564	0.971	0.934	2.72E-78	3.91E-74	mCD301b+ DTR
Ltc4s	0.4449	0.627	0.516	4.63E-33	6.65E-29	mCD301b+ DTR
Zfp36	0.4449	0.876	0.811	9.88E-47	1.42E-42	mCD301b+ DTR
Jun	0.4405	0.797	0.763	1.00E-28	1.44E-24	mCD301b+ DTR
Id2	0.4290	0.989	0.976	3.85E-60	5.53E-56	mCD301b+ DTR
Atf3	0.4216	0.391	0.298	2.53E-30	3.64E-26	mCD301b+ DTR
Eif3e	0.4132	0.921	0.884	4.08E-63	5.86E-59	mCD301b+ DTR
Rps9	0.4120	0.999	1	2.05E-126	2.95E-122	mCD301b+ DTR
Rel	0.4112	0.83	0.769	3.68E-44	5.30E-40	mCD301b+ DTR
Zfp36l1	0.4028	0.968	0.936	6.98E-53	1.00E-48	mCD301b+ DTR
Ccl17	-1.5065	0.877	0.652	1.41E-99	2.03E-95	mCD301b- DTR
H2-Ab1	-1.4184	0.961	0.843	4.19E-151	6.03E-147	mCD301b- DTR
H2-Eb1	-1.1105	0.955	0.792	3.02E-110	4.34E-106	mCD301b- DTR
Tagln2	-1.1070	0.99	0.736	2.51E-236	3.62E-232	mCD301b- DTR
Ccnd2	-1.0573	0.539	0.121	2.07E-112	2.98E-108	mCD301b- DTR
Cd74	-1.0364	0.999	0.996	3.29E-143	4.73E-139	mCD301b- DTR
H2-Aa	-1.0312	0.981	0.894	3.12E-114	4.49E-110	mCD301b- DTR
Isg15	-1.0082	0.569	0.232	1.23E-84	1.76E-80	mCD301b- DTR
AA467197	-0.9998	0.751	0.306	3.18E-125	4.58E-121	mCD301b- DTR
Fabp5	-0.9955	0.982	0.942	1.86E-126	2.68E-122	mCD301b- DTR
Anxa2	-0.9913	0.979	0.814	5.63E-191	8.09E-187	mCD301b- DTR
Cd40	-0.9805	0.771	0.34	3.95E-125	5.68E-121	mCD301b- DTR
Ccl22	-0.9736	0.979	0.894	1.23E-93	1.76E-89	mCD301b- DTR
Lgals1	-0.9487	0.882	0.592	4.07E-130	5.86E-126	mCD301b- DTR
Cst3	-0.9086	1	0.999	1.24E-209	1.78E-205	mCD301b- DTR
H2-DMb2	-0.8043	0.482	0.144	7.32E-70	1.05E-65	mCD301b- DTR
Cd1d1	-0.7898	0.564	0.186	1.90E-91	2.74E-87	mCD301b- DTR
Myl12a	-0.7746	0.974	0.826	8.15E-150	1.17E-145	mCD301b- DTR

gene	avg_logFC	pct.1	pct.2	p_val	p_val_adj	cluster
Coro1a	-0.7700	0.856	0.56	2.90E-118	4.17E-114	mCD301b- DTR
H2-DMa	-0.7544	0.668	0.299	3.34E-87	4.81E-83	mCD301b- DTR
Cd86	-0.6969	0.817	0.508	5.97E-77	8.58E-73	mCD301b- DTR
Actb	-0.6829	1	0.999	4.96E-165	7.13E-161	mCD301b- DTR
Tnfrsf4	-0.6797	0.586	0.294	2.69E-59	3.86E-55	mCD301b- DTR
Glipr2	-0.6774	0.953	0.758	5.15E-91	7.41E-87	mCD301b- DTR
Bcl2a1d	-0.6749	0.975	0.847	1.95E-128	2.81E-124	mCD301b- DTR
Pfn1	-0.6694	1	0.994	1.04E-196	1.49E-192	mCD301b- DTR
Cnn2	-0.6652	0.968	0.762	6.43E-121	9.25E-117	mCD301b- DTR
S100a10	-0.6535	0.728	0.557	3.74E-50	5.38E-46	mCD301b- DTR
Irf8	-0.6488	0.876	0.722	1.85E-52	2.66E-48	mCD301b- DTR
Cd1d2	-0.6319	0.384	0.082	1.70E-68	2.45E-64	mCD301b- DTR
Bcl2a1b	-0.6266	0.993	0.956	5.15E-128	7.40E-124	mCD301b- DTR
Cfl1	-0.6159	0.994	0.934	2.16E-136	3.11E-132	mCD301b- DTR
Cd82	-0.6052	0.516	0.223	2.34E-53	3.37E-49	mCD301b- DTR
Bcl2a1a	-0.5989	0.893	0.718	5.60E-64	8.05E-60	mCD301b- DTR
Tnfsf9	-0.5973	0.342	0.069	7.65E-59	1.10E-54	mCD301b- DTR
Ctsz	-0.5914	0.987	0.927	3.40E-116	4.89E-112	mCD301b- DTR
Il4i1	-0.5856	0.949	0.791	1.41E-76	2.03E-72	mCD301b- DTR
Napsa	-0.5805	0.601	0.296	3.54E-67	5.09E-63	mCD301b- DTR
Myl6	-0.5784	1	0.982	1.92E-130	2.77E-126	mCD301b- DTR
Vwa5a	-0.5750	0.657	0.341	6.07E-64	8.73E-60	mCD301b- DTR
Cd70	-0.5683	0.265	0.035	3.93E-60	5.65E-56	mCD301b- DTR
S100a11	-0.5608	0.984	0.943	2.10E-81	3.02E-77	mCD301b- DTR
Txn1	-0.5604	0.986	0.904	1.46E-78	2.11E-74	mCD301b- DTR
Ifi30	-0.5571	0.966	0.86	2.53E-82	3.64E-78	mCD301b- DTR
Gapdh	-0.5555	0.966	0.829	7.99E-86	1.15E-81	mCD301b- DTR
Srgn	-0.5510	0.999	0.984	1.84E-131	2.64E-127	mCD301b- DTR
Cd81	-0.5477	0.45	0.269	7.53E-30	1.08E-25	mCD301b- DTR
Arpc2	-0.5379	0.99	0.929	4.15E-116	5.96E-112	mCD301b- DTR
Gpr183	-0.5299	0.392	0.118	1.20E-48	1.72E-44	mCD301b- DTR
Calm1	-0.5297	1	0.998	6.22E-160	8.95E-156	mCD301b- DTR
Arpc5	-0.5296	0.966	0.849	5.11E-92	7.35E-88	mCD301b- DTR
Gngt2	-0.5279	0.79	0.508	1.54E-52	2.22E-48	mCD301b- DTR
Lrrc58	-0.5189	0.924	0.718	1.04E-78	1.50E-74	mCD301b- DTR
Tap1	-0.5144	0.792	0.484	7.04E-70	1.01E-65	mCD301b- DTR
Apol7c	-0.5121	0.702	0.573	1.64E-16	2.36E-12	mCD301b- DTR
Glrx	-0.5079	0.5	0.214	5.22E-46	7.51E-42	mCD301b- DTR
Wnk1	-0.5076	0.958	0.801	3.32E-71	4.78E-67	mCD301b- DTR
Emp3	-0.5068	0.714	0.421	3.63E-62	5.22E-58	mCD301b- DTR
Arpc1b	-0.5006	0.983	0.941	6.55E-101	9.42E-97	mCD301b- DTR
Ccnd1	-0.4998	0.325	0.053	5.51E-62	7.93E-58	mCD301b- DTR
Necap2	-0.4976	0.812	0.502	8.42E-70	1.21E-65	mCD301b- DTR
S100a6	-0.4969	0.969	0.912	4.71E-55	6.77E-51	mCD301b- DTR
Arpc4	-0.4968	0.867	0.613	3.91E-70	5.63E-66	mCD301b- DTR
Cd302	-0.4958	0.483	0.184	9.18E-54	1.32E-49	mCD301b- DTR
Clic4	-0.4861	0.93	0.743	3.13E-66	4.50E-62	mCD301b- DTR
Cotl1	-0.4833	0.576	0.3	1.02E-56	1.47E-52	mCD301b- DTR
Calm3	-0.4775	0.891	0.676	4.98E-69	7.16E-65	mCD301b- DTR
Tspo	-0.4734	0.983	0.949	4.00E-69	5.76E-65	mCD301b- DTR
Ggh	-0.4689	0.532	0.216	2.06E-63	2.96E-59	mCD301b- DTR
Rnaset2a	-0.4664	0.606	0.349	8.60E-37	1.24E-32	mCD301b- DTR

gene	avg_logFC	pct.1	pct.2	p_val	p_val_adj	cluster
Lgals3	-0.4585	0.689	0.447	6.62E-38	9.53E-34	mCD301b- DTR
Ifi27l2a	-0.4529	0.536	0.296	1.17E-36	1.68E-32	mCD301b- DTR
Fscn1	-0.4527	0.995	0.989	2.28E-74	3.28E-70	mCD301b- DTR
Cd63	-0.4471	0.99	0.939	2.27E-58	3.26E-54	mCD301b- DTR
Gpx1	-0.4466	0.872	0.662	1.20E-48	1.72E-44	mCD301b- DTR
Nans	-0.4459	0.797	0.53	6.02E-49	8.66E-45	mCD301b- DTR
Igsf8	-0.4456	0.466	0.169	7.55E-55	1.09E-50	mCD301b- DTR
Tmem39a	-0.4427	0.741	0.441	2.74E-52	3.93E-48	mCD301b- DTR
Tpm4	-0.4425	0.906	0.693	3.99E-58	5.74E-54	mCD301b- DTR
Ube2l6	-0.4362	0.874	0.671	6.81E-47	9.79E-43	mCD301b- DTR
Tmbim6	-0.4359	0.933	0.77	2.10E-60	3.01E-56	mCD301b- DTR
Pkib	-0.4342	0.521	0.356	1.30E-20	1.87E-16	mCD301b- DTR
Map2k1	-0.4338	0.6	0.262	1.05E-59	1.51E-55	mCD301b- DTR
Inpp5b	-0.4319	0.455	0.171	6.51E-49	9.36E-45	mCD301b- DTR
Idi1	-0.4249	0.708	0.421	6.04E-43	8.68E-39	mCD301b- DTR
Ebi3	-0.4246	0.384	0.131	1.84E-41	2.65E-37	mCD301b- DTR
Tap2	-0.4246	0.68	0.358	2.98E-52	4.29E-48	mCD301b- DTR
Crip1	-0.4244	0.999	1	2.84E-61	4.08E-57	mCD301b- DTR
Ifitm2	-0.4242	0.862	0.681	6.71E-41	9.65E-37	mCD301b- DTR
Vasp	-0.4211	0.662	0.38	2.86E-48	4.11E-44	mCD301b- DTR
Vcp	-0.4108	0.854	0.617	2.75E-49	3.96E-45	mCD301b- DTR
Tnfrsf18	-0.4101	0.501	0.229	2.56E-42	3.68E-38	mCD301b- DTR
Tyrobp	-0.4077	0.966	0.885	1.26E-42	1.81E-38	mCD301b- DTR
Serpinb9	-0.4068	0.928	0.807	2.19E-35	3.15E-31	mCD301b- DTR
Reep5	-0.4051	0.771	0.503	2.27E-45	3.26E-41	mCD301b- DTR
Serpinb1a	-0.4051	0.477	0.367	1.32E-09	1.90E-05	mCD301b- DTR
Psme2	-0.4017	1	0.99	1.20E-126	1.73E-122	mCD301b- DTR

(**B**)

gene	avg_logFC	pct.1	pct.2	p_val	p_val_adj	cluster
Klf2	1.5021	0.759	0.38	1.1E-73	1.7E-69	mCD301b- tdLN
Fos	0.7575	0.712	0.513	7.4E-25	1.1E-20	mCD301b- tdLN
Eno3	0.7260	0.894	0.727	1.3E-45	1.9E-41	mCD301b- tdLN
Dusp2	0.6617	0.514	0.264	5.2E-21	7.8E-17	mCD301b- tdLN
Zmynd15	0.6497	0.755	0.577	7.5E-22	1.1E-17	mCD301b- tdLN
Ccl5	0.6393	1	0.999	2.5E-24	3.7E-20	mCD301b- tdLN
Apol7c	0.6309	0.774	0.607	2.2E-18	3.2E-14	mCD301b- tdLN
Cxcl1	0.6066	0.2	0.121	4.8E-06	7.1E-02	mCD301b- tdLN
Tmem176a	0.5765	0.998	0.977	4.7E-64	7.1E-60	mCD301b- tdLN
Etv3	0.5638	0.858	0.738	3.1E-40	4.6E-36	mCD301b- tdLN
Icosl	0.5620	0.441	0.208	1.2E-23	1.7E-19	mCD301b- tdLN
Klf6	0.5600	0.988	0.984	1.8E-42	2.7E-38	mCD301b- tdLN
Zfp36	0.5552	0.875	0.805	3.5E-29	5.3E-25	mCD301b- tdLN
Gnl2	0.5491	0.698	0.539	3.3E-22	5.0E-18	mCD301b- tdLN
Serinc3	0.5376	0.413	0.147	3.4E-33	5.0E-29	mCD301b- tdLN
Jund	0.5271	0.814	0.731	3.1E-26	4.6E-22	mCD301b- tdLN
Junb	0.5216	0.958	0.941	7.3E-30	1.1E-25	mCD301b- tdLN
Ppp1r15a	0.5207	0.896	0.763	3.2E-33	4.9E-29	mCD301b- tdLN

gene	avg_logFC	pct.1	pct.2	p_val	p_val_adj	cluster
Cited2	0.5201	0.441	0.344	2.0E-18	3.0E-14	mCD301b- tdLN
Tspan3	0.5197	0.941	0.908	1.2E-26	1.8E-22	mCD301b- tdLN
Tmem176b	0.5169	0.993	0.988	2.6E-61	3.9E-57	mCD301b- tdLN
Jun	0.5157	0.873	0.825	5.0E-19	7.4E-15	mCD301b- tdLN
H3f3b	0.5020	1	0.999	6.9E-45	1.0E-40	mCD301b- tdLN
Fosb	0.4781	0.351	0.179	8.5E-20	1.3E-15	mCD301b- tdLN
Tnfrsf1b	0.4753	0.509	0.366	1.1E-28	1.6E-24	mCD301b- tdLN
Tbc1d4	0.4734	0.976	0.949	1.7E-34	2.5E-30	mCD301b- tdLN
Klf4	0.4693	0.377	0.243	6.8E-16	1.0E-11	mCD301b- tdLN
Tubb2a	0.4654	0.686	0.545	6.4E-19	9.6E-15	mCD301b- tdLN
Hist1h2bc	0.4648	0.491	0.406	4.1E-11	6.2E-07	mCD301b- tdLN
Pmaip1	0.4590	0.767	0.65	4.7E-19	7.0E-15	mCD301b- tdLN
Pygl	0.4589	0.392	0.181	3.5E-19	5.2E-15	mCD301b- tdLN
Nabp1	0.4562	0.488	0.329	1.9E-18	2.8E-14	mCD301b- tdLN
Tmem158	0.4561	0.222	0.042	1.0E-19	1.6E-15	mCD301b- tdLN
Tubb2b	0.4545	0.368	0.185	2.3E-12	3.5E-08	mCD301b- tdLN
Phf11a	0.4448	0.446	0.272	5.5E-17	8.2E-13	mCD301b- tdLN
Birc2	0.4432	0.858	0.795	4.2E-24	6.3E-20	mCD301b- tdLN
Lmo4	0.4319	0.264	0.072	4.6E-20	6.9E-16	mCD301b- tdLN
Rgs1	0.4314	0.96	0.957	6.3E-18	9.4E-14	mCD301b- tdLN
Malat1	0.4304	1	0.999	3.9E-44	5.8E-40	mCD301b- tdLN
Mxd1	0.4213	0.835	0.78	5.9E-20	8.8E-16	mCD301b- tdLN
H2-Q4	0.4170	0.868	0.789	1.6E-25	2.4E-21	mCD301b- tdLN
Ndnl2	0.4162	0.575	0.478	5.5E-18	8.3E-14	mCD301b- tdLN
Dusp1	0.4157	0.955	0.922	3.2E-18	4.8E-14	mCD301b- tdLN
Nmrk1	0.4156	0.406	0.223	2.1E-20	3.1E-16	mCD301b- tdLN
Phf11b	0.4153	0.785	0.699	6.3E-21	9.5E-17	mCD301b- tdLN
Rrad	0.4094	0.257	0.23	2.3E-15	3.4E-11	mCD301b- tdLN
Atf3	0.4087	0.417	0.318	1.3E-10	1.9E-06	mCD301b- tdLN
Tmem123	0.4025	1	0.999	6.6E-42	9.9E-38	mCD301b- tdLN
Ucp2	0.3998	0.731	0.64	1.2E-20	1.8E-16	mCD301b- tdLN
Spint2	0.3996	0.96	0.948	6.9E-31	1.0E-26	mCD301b- tdLN
Slc38a2	0.3961	0.514	0.367	4.2E-18	6.3E-14	mCD301b- tdLN
Frmd4a	0.3918	0.509	0.382	5.6E-17	8.4E-13	mCD301b- tdLN
Skil	0.3907	0.469	0.305	1.6E-14	2.4E-10	mCD301b- tdLN
Bhlhe40	0.3828	0.726	0.679	1.7E-20	2.5E-16	mCD301b- tdLN
Rcsd1	0.3722	0.88	0.776	6.1E-18	9.1E-14	mCD301b- tdLN
Apol10b	0.3713	0.262	0.159	2.9E-17	4.3E-13	mCD301b- tdLN
Stard7	0.3657	0.491	0.335	1.4E-17	2.1E-13	mCD301b- tdLN
Ccnd1	0.3644	0.42	0.329	7.6E-09	1.1E-04	mCD301b- tdLN
Rgs2	0.3644	0.314	0.195	7.5E-12	1.1E-07	mCD301b- tdLN
Epsti1	0.3626	1	0.991	8.3E-20	1.2E-15	mCD301b- tdLN
H3f3a	0.3606	0.995	0.988	4.7E-28	7.1E-24	mCD301b- tdLN
Tnfrsf4	0.3594	0.785	0.695	1.5E-09	2.3E-05	mCD301b- tdLN
Pim1	0.3571	0.913	0.909	4.0E-18	5.9E-14	mCD301b- tdLN
Btg2	0.3528	0.601	0.499	9.4E-11	1.4E-06	mCD301b- tdLN
Tnfaip3	0.3464	0.568	0.499	1.2E-17	1.8E-13	mCD301b- tdLN
Ostf1	0.3437	0.981	0.99	4.5E-24	6.7E-20	mCD301b- tdLN
Csrnp1	0.3423	0.41	0.327	4.0E-20	6.0E-16	mCD301b- tdLN
Chka	0.3382	0.42	0.319	4.0E-11	6.0E-07	mCD301b- tdLN
Ankrd35	0.3377	0.368	0.253	2.1E-13	3.1E-09	mCD301b- tdLN
Plxnc1	0.3377	0.58	0.481	1.2E-18	1.8E-14	mCD301b- tdLN

gene	avg_logFC	pct.1	pct.2	p_val	p_val_adj	cluster
Cd83	0.3376	0.91	0.922	3.6E-17	5.4E-13	mCD301b- tdLN
Tmem19	0.3331	0.521	0.445	9.4E-17	1.4E-12	mCD301b- tdLN
Fam53b	0.3309	0.524	0.389	9.2E-11	1.4E-06	mCD301b- tdLN
Kmt2e	0.3293	0.448	0.371	1.8E-18	2.7E-14	mCD301b- tdLN
Arhgap22	0.3276	0.597	0.53	2.8E-16	4.2E-12	mCD301b- tdLN
Kctd12	0.3263	0.311	0.207	8.2E-13	1.2E-08	mCD301b- tdLN
H2-K1	0.3241	1	1	4.0E-39	6.0E-35	mCD301b- tdLN
Zfp36l1	0.3220	0.955	0.942	6.1E-15	9.1E-11	mCD301b- tdLN
H2-D1	0.3212	1	1	4.9E-51	7.4E-47	mCD301b- tdLN
Creg1	0.3166	0.526	0.426	1.3E-11	1.9E-07	mCD301b- tdLN
Htra2	0.3142	0.764	0.74	1.4E-21	2.1E-17	mCD301b- tdLN
Il1b	0.3135	0.241	0.179	3.0E-04	1.0E+00	mCD301b- tdLN
Sec11c	0.3121	0.842	0.803	4.7E-14	7.0E-10	mCD301b- tdLN
Nfkbia	0.3119	0.995	0.996	4.2E-15	6.3E-11	mCD301b- tdLN
H2-Eb2	0.3097	0.283	0.165	1.6E-10	2.4E-06	mCD301b- tdLN
Bmp2k	0.3095	0.71	0.678	1.4E-16	2.1E-12	mCD301b- tdLN
Man1a	0.3085	0.363	0.23	5.0E-12	7.5E-08	mCD301b- tdLN
Rap2b	0.3055	0.783	0.73	2.4E-14	3.6E-10	mCD301b- tdLN
Laptm5	0.3046	0.767	0.718	4.0E-13	6.0E-09	mCD301b- tdLN
Cers6	0.3042	0.439	0.376	2.6E-16	3.9E-12	mCD301b- tdLN
Relb	0.3033	0.976	0.98	2.1E-20	3.1E-16	mCD301b- tdLN
Rassf4	0.3025	0.559	0.481	1.5E-13	2.2E-09	mCD301b- tdLN
Glipr1	0.3014	0.443	0.312	2.8E-10	4.2E-06	mCD301b- tdLN
Mthfsl	0.2972	0.71	0.636	2.8E-12	4.2E-08	mCD301b- tdLN
Ccl17	2.1187	0.798	0.248	2.4E-86	3.5E-82	mCD301b- DTR
Ccl22	1.3770	0.941	0.63	6.7E-72	1.0E-67	mCD301b- DTR
Ccl24	1.1418	0.202	0.002	2.2E-29	3.2E-25	mCD301b- DTR
Lgals1	1.0860	0.854	0.465	1.0E-67	1.5E-63	mCD301b- DTR
Cd1d2	0.9156	0.526	0.066	1.9E-63	2.8E-59	mCD301b- DTR
AA467197	0.8983	0.769	0.349	3.1E-55	4.6E-51	mCD301b- DTR
Gm13546	0.8761	0.539	0.12	3.8E-54	5.6E-50	mCD301b- DTR
Pkib	0.8452	0.432	0.087	1.6E-39	2.3E-35	mCD301b- DTR
Ramp3	0.8316	0.705	0.321	2.1E-45	3.2E-41	mCD301b- DTR
Cytip	0.7920	0.84	0.465	1.0E-52	1.5E-48	mCD301b- DTR
S100a10	0.7663	0.61	0.29	2.0E-28	3.0E-24	mCD301b- DTR
Ccnd2	0.7045	0.607	0.323	2.5E-24	3.8E-20	mCD301b- DTR
Capg	0.6362	0.519	0.196	4.6E-30	6.9E-26	mCD301b- DTR
Rps27l	0.6274	0.994	0.95	2.7E-53	4.0E-49	mCD301b- DTR
Fabp5	0.6111	0.978	0.955	3.7E-25	5.6E-21	mCD301b- DTR
Slc27a3	0.5627	0.311	0.042	2.1E-30	3.1E-26	mCD301b- DTR
Cst3	0.5446	1	0.995	9.8E-44	1.5E-39	mCD301b- DTR
Tnip3	0.5392	0.512	0.193	1.3E-25	2.0E-21	mCD301b- DTR
Vim	0.5335	0.952	0.856	1.4E-17	2.2E-13	mCD301b- DTR
Stat4	0.5055	0.595	0.283	1.7E-24	2.5E-20	mCD301b- DTR
Amica1	0.4985	0.353	0.075	5.1E-28	7.6E-24	mCD301b- DTR
Cd86	0.4835	0.809	0.517	2.1E-24	3.2E-20	mCD301b- DTR
Cnn3	0.4734	0.473	0.165	6.1E-27	9.1E-23	mCD301b- DTR
Gsn	0.4592	0.366	0.108	1.5E-21	2.3E-17	mCD301b- DTR
H2afy	0.4539	0.772	0.436	2.9E-29	4.3E-25	mCD301b- DTR
Got1	0.4445	0.409	0.156	1.3E-18	1.9E-14	mCD301b- DTR
Ptpn1	0.4438	0.639	0.349	5.5E-25	8.2E-21	mCD301b- DTR
Cd302	0.4429	0.406	0.151	3.8E-20	5.7E-16	mCD301b- DTR

gene	avg_logFC	pct.1	pct.2	p_val	p_val_adj	cluster
Pdcd1lg2	0.4404	0.506	0.191	4.6E-25	6.9E-21	mCD301b- DTR
Plgrkt	0.4396	0.676	0.41	3.1E-20	4.7E-16	mCD301b- DTR
Serpinb6b	0.4262	0.981	0.908	9.2E-25	1.4E-20	mCD301b- DTR
Rps6	0.4028	0.997	0.988	1.2E-35	1.8E-31	mCD301b- DTR
Tyms	0.4027	0.353	0.064	6.3E-30	9.4E-26	mCD301b- DTR
Serpinb1a	0.3920	0.403	0.283	2.6E-04	1.0E+00	mCD301b- DTR
Glipr2	0.3903	0.965	0.875	9.9E-20	1.5E-15	mCD301b- DTR
Stat1	0.3889	0.788	0.517	7.3E-21	1.1E-16	mCD301b- DTR
Tspo	0.3887	0.994	0.969	2.7E-27	4.0E-23	mCD301b- DTR
Mkrn1	0.3865	0.675	0.382	1.9E-21	2.8E-17	mCD301b- DTR
Gapdh	0.3813	0.951	0.844	1.3E-18	1.9E-14	mCD301b- DTR
Coro1a	0.3805	0.837	0.632	5.2E-16	7.8E-12	mCD301b- DTR
Fkbp1a	0.3764	0.611	0.344	8.2E-19	1.2E-14	mCD301b- DTR
Selm	0.3737	0.665	0.491	5.7E-08	8.6E-04	mCD301b- DTR
Myl12a	0.3625	0.961	0.92	8.6E-17	1.3E-12	mCD301b- DTR
Rps11	0.3612	1	0.998	5.1E-55	7.7E-51	mCD301b- DTR
Rps4x	0.3597	0.997	0.96	1.4E-29	2.0E-25	mCD301b- DTR
H2-DMa	0.3597	0.655	0.429	3.1E-12	4.6E-08	mCD301b- DTR
Psma6	0.3591	0.866	0.71	8.4E-18	1.3E-13	mCD301b- DTR
Txn1	0.3563	0.978	0.917	2.3E-16	3.5E-12	mCD301b- DTR
Nostrin	0.3558	0.772	0.524	2.7E-17	4.0E-13	mCD301b- DTR
Acot7	0.3555	0.458	0.205	8.2E-17	1.2E-12	mCD301b- DTR
Lyz2	0.3503	0.608	0.384	7.0E-13	1.0E-08	mCD301b- DTR
Syngr2	0.3494	0.991	0.965	1.6E-21	2.4E-17	mCD301b- DTR
Actg1	0.3483	1	1	1.2E-36	1.9E-32	mCD301b- DTR
Lcp1	0.3477	0.829	0.653	1.1E-13	1.7E-09	mCD301b- DTR
Rpl12	0.3447	0.873	0.684	4.1E-17	6.1E-13	mCD301b- DTR
Rab8b	0.3442	0.738	0.493	4.7E-16	7.0E-12	mCD301b- DTR
Lactb	0.3440	0.764	0.542	7.4E-15	1.1E-10	mCD301b- DTR
Ehd1	0.3408	0.506	0.267	3.9E-14	5.9E-10	mCD301b- DTR
Procr	0.3356	0.382	0.16	3.9E-14	5.9E-10	mCD301b- DTR
Lgals3	0.3335	0.655	0.453	1.9E-11	2.9E-07	mCD301b- DTR
Cd9	0.3330	0.587	0.354	7.9E-13	1.2E-08	mCD301b- DTR
Slc25a3	0.3318	0.876	0.703	2.0E-17	3.0E-13	mCD301b- DTR
Rpl10a	0.3314	0.939	0.854	1.4E-14	2.0E-10	mCD301b- DTR
Clta	0.3307	0.962	0.87	6.9E-18	1.0E-13	mCD301b- DTR
S100a6	0.3307	0.962	0.875	3.1E-15	4.7E-11	mCD301b- DTR
Serpina3g	0.3298	0.543	0.302	2.5E-14	3.7E-10	mCD301b- DTR
Eno1	0.3287	0.519	0.271	1.3E-15	2.0E-11	mCD301b- DTR
Tnfaip8	0.3280	0.682	0.448	4.7E-14	7.0E-10	mCD301b- DTR
Lrrc58	0.3278	0.91	0.764	3.3E-16	4.9E-12	mCD301b- DTR
Gpx1	0.3258	0.835	0.608	3.4E-16	5.0E-12	mCD301b- DTR
Zbp1	0.3254	0.457	0.219	6.9E-15	1.0E-10	mCD301b- DTR
Gdi2	0.3244	0.883	0.708	3.9E-17	5.8E-13	mCD301b- DTR
Cfl1	0.3232	0.994	0.955	1.3E-19	1.9E-15	mCD301b- DTR
Srgn	0.3225	1	0.991	4.9E-25	7.3E-21	mCD301b- DTR
Rab14	0.3221	0.832	0.59	1.6E-18	2.4E-14	mCD301b- DTR
Glrx	0.3215	0.62	0.389	1.0E-12	1.5E-08	mCD301b- DTR
Eva1b	0.3184	0.592	0.356	1.7E-13	2.5E-09	mCD301b- DTR
Cd80	0.3120	0.402	0.203	7.1E-12	1.1E-07	mCD301b- DTR
Prps1	0.3090	0.289	0.101	2.3E-17	3.4E-13	mCD301b- DTR
Tspan13	0.3078	0.658	0.432	1.4E-12	2.1E-08	mCD301b- DTR

gene	avg_logFC	pct.1	pct.2	p_val	p_val_adj	cluster
Rpl10	0.3076	1	0.976	3.5E-28	5.3E-24	mCD301b- DTR
Rps8	0.3045	0.965	0.915	5.8E-15	8.7E-11	mCD301b- DTR
Rps17	0.3029	0.883	0.731	4.5E-13	6.8E-09	mCD301b- DTR
Arpc1b	0.3010	0.996	0.965	1.1E-23	1.7E-19	mCD301b- DTR
Cxcl1	1.3860	0.437	0.162	3.8E-56	5.6E-52	mCD301b+ tdLN
Klf2	1.2722	0.785	0.406	3.3E-111	4.9E-107	mCD301b+ tdLN
Fxyd2	0.9176	0.577	0.294	2.1E-57	3.2E-53	mCD301b+ tdLN
Clu	0.7647	0.684	0.513	5.9E-34	8.8E-30	mCD301b+ tdLN
Tmem158	0.6672	0.346	0.109	2.0E-43	3.0E-39	mCD301b+ tdLN
Tspan3	0.6556	0.938	0.836	2.0E-68	3.0E-64	mCD301b+ tdLN
Fos	0.6494	0.842	0.683	1.2E-38	1.8E-34	mCD301b+ tdLN
Dusp2	0.6481	0.526	0.277	6.3E-35	9.5E-31	mCD301b+ tdLN
Glipr1	0.6254	0.692	0.414	4.6E-65	6.8E-61	mCD301b+ tdLN
Apol7c	0.6138	0.87	0.698	2.6E-51	3.9E-47	mCD301b+ tdLN
Fosb	0.6039	0.535	0.291	1.8E-42	2.7E-38	mCD301b+ tdLN
Eno3	0.5701	0.714	0.526	1.2E-48	1.7E-44	mCD301b+ tdLN
Atf3	0.5360	0.635	0.394	1.0E-35	1.5E-31	mCD301b+ tdLN
Mfge8	0.5262	0.431	0.279	3.0E-21	4.5E-17	mCD301b+ tdLN
Ppp1r15a	0.5217	0.854	0.753	1.1E-55	1.6E-51	mCD301b+ tdLN
H2-M2	0.5135	0.669	0.598	5.0E-21	7.5E-17	mCD301b+ tdLN
Gnl2	0.4904	0.525	0.31	4.1E-32	6.1E-28	mCD301b+ tdLN
Bhlhe40	0.4848	0.715	0.574	2.5E-37	3.7E-33	mCD301b+ tdLN
Creg1	0.4590	0.608	0.4	1.8E-36	2.6E-32	mCD301b+ tdLN
Il4i1	0.4543	0.863	0.837	6.1E-38	9.0E-34	mCD301b+ tdLN
Cxcl2	0.4524	0.314	0.17	6.4E-13	9.6E-09	mCD301b+ tdLN
Etv3	0.4512	0.914	0.805	2.4E-47	3.5E-43	mCD301b+ tdLN
Tnfaip3	0.4505	0.69	0.539	8.9E-36	1.3E-31	mCD301b+ tdLN
Hspa1a	0.4471	0.264	0.137	2.8E-13	4.3E-09	mCD301b+ tdLN
Rap2b	0.4451	0.769	0.657	1.5E-43	2.2E-39	mCD301b+ tdLN
Junb	0.4414	0.954	0.939	4.1E-43	6.1E-39	mCD301b+ tdLN
Tubb2a	0.4342	0.521	0.338	1.8E-28	2.7E-24	mCD301b+ tdLN
Lmo4	0.4320	0.382	0.199	8.2E-27	1.2E-22	mCD301b+ tdLN
Ier2	0.4314	0.545	0.37	3.2E-21	4.7E-17	mCD301b+ tdLN
M1ap	0.4239	0.388	0.205	6.9E-26	1.0E-21	mCD301b+ tdLN
Ehf	0.4237	0.371	0.163	2.5E-28	3.7E-24	mCD301b+ tdLN
Cdc42ep3	0.4220	0.732	0.674	3.2E-31	4.8E-27	mCD301b+ tdLN
Tmem176b	0.4191	0.981	0.962	3.6E-67	5.4E-63	mCD301b+ tdLN
Pvr	0.4168	0.468	0.265	6.4E-30	9.6E-26	mCD301b+ tdLN
2610528A11Rik	0.4156	0.138	0.046	3.7E-13	5.6E-09	mCD301b+ tdLN
Evi2a	0.4144	0.326	0.129	3.2E-33	4.8E-29	mCD301b+ tdLN
Tmem176a	0.4122	0.971	0.936	6.0E-56	8.9E-52	mCD301b+ tdLN
Rgs2	0.4069	0.388	0.217	2.9E-20	4.3E-16	mCD301b+ tdLN
Jund	0.4031	0.874	0.818	3.7E-33	5.5E-29	mCD301b+ tdLN
Cited2	0.4021	0.479	0.353	8.3E-18	1.2E-13	mCD301b+ tdLN
Skil	0.4015	0.532	0.352	6.1E-28	9.2E-24	mCD301b+ tdLN
Cd44	0.3958	0.767	0.662	2.3E-29	3.4E-25	mCD301b+ tdLN
Jun	0.3954	0.776	0.715	2.4E-16	3.6E-12	mCD301b+ tdLN
Hist1h1c	0.3933	0.532	0.412	3.4E-18	5.1E-14	mCD301b+ tdLN
Egr1	0.3927	0.229	0.069	5.3E-23	8.0E-19	mCD301b+ tdLN
Gpr183	0.3881	0.311	0.171	3.7E-15	5.5E-11	mCD301b+ tdLN
Nfkbia	0.3849	0.99	0.988	4.8E-28	7.1E-24	mCD301b+ tdLN
Klf4	0.3773	0.435	0.271	1.1E-17	1.7E-13	mCD301b+ tdLN

gene	avg_logFC	pct.1	pct.2	p_val	p_val_adj	cluster
Tubb6	0.3725	0.4	0.267	6.5E-25	9.8E-21	mCD301b+ tdLN
Nfkbiz	0.3702	0.593	0.469	7.8E-23	1.2E-18	mCD301b+ tdLN
Rrad	0.3659	0.349	0.242	1.1E-10	1.7E-06	mCD301b+ tdLN
Klf6	0.3643	0.957	0.941	1.6E-25	2.4E-21	mCD301b+ tdLN
Ccl9	0.3629	0.275	0.154	1.1E-11	1.7E-07	mCD301b+ tdLN
Hist1h2bc	0.3625	0.632	0.506	8.0E-14	1.2E-09	mCD301b+ tdLN
Ucp2	0.3613	0.793	0.714	1.1E-35	1.6E-31	mCD301b+ tdLN
Cd83	0.3581	0.875	0.867	2.4E-28	3.6E-24	mCD301b+ tdLN
Mycbp2	0.3573	0.706	0.565	2.4E-26	3.6E-22	mCD301b+ tdLN
Sat1	0.3566	0.915	0.861	2.0E-30	3.0E-26	mCD301b+ tdLN
Gm10116	0.3564	0.594	0.449	8.6E-31	1.3E-26	mCD301b+ tdLN
Rhob	0.3546	0.328	0.149	4.8E-23	7.2E-19	mCD301b+ tdLN
Ftl1	0.3539	0.999	1	1.4E-43	2.1E-39	mCD301b+ tdLN
Pmaip1	0.3498	0.803	0.689	3.2E-19	4.8E-15	mCD301b+ tdLN
Basp1	0.3408	0.864	0.812	3.2E-29	4.8E-25	mCD301b+ tdLN
Zfp36	0.3382	0.903	0.857	8.4E-25	1.3E-20	mCD301b+ tdLN
Fgl2	0.3321	0.408	0.286	2.0E-15	3.0E-11	mCD301b+ tdLN
Lmna	0.3315	0.391	0.25	5.1E-21	7.6E-17	mCD301b+ tdLN
Vcam1	0.3265	0.286	0.136	3.8E-19	5.7E-15	mCD301b+ tdLN
Tnf	0.3255	0.208	0.081	4.7E-18	7.1E-14	mCD301b+ tdLN
Zeb2	0.3235	0.455	0.328	9.8E-20	1.5E-15	mCD301b+ tdLN
Galnt12	0.3229	0.421	0.255	1.4E-22	2.2E-18	mCD301b+ tdLN
Birc2	0.3175	0.834	0.787	4.8E-25	7.1E-21	mCD301b+ tdLN
Ostf1	0.3163	0.942	0.942	6.3E-32	9.4E-28	mCD301b+ tdLN
Brk1	0.3143	0.926	0.912	2.8E-29	4.2E-25	mCD301b+ tdLN
Adm	0.3135	0.215	0.091	6.0E-20	9.0E-16	mCD301b+ tdLN
Vrk2	0.3076	0.411	0.274	1.8E-19	2.8E-15	mCD301b+ tdLN
Anxa3	0.3066	0.976	0.968	3.1E-37	4.6E-33	mCD301b+ tdLN
Dkkl1	0.3040	0.229	0.071	4.0E-25	6.0E-21	mCD301b+ tdLN
Adgre4	0.3017	0.159	0.016	1.6E-32	2.4E-28	mCD301b+ tdLN
Il1b	0.3017	0.27	0.227	1.6E-04	1.0E+00	mCD301b+ tdLN
Ptgs2	0.3012	0.325	0.198	2.7E-09	4.0E-05	mCD301b+ tdLN
Rps3a1	0.3010	0.998	1	2.2E-53	3.3E-49	mCD301b+ tdLN
Tmem123	0.3001	0.998	0.995	7.0E-34	1.1E-29	mCD301b+ tdLN
Gm13546	1.3265	0.653	0.11	8.2E-164	1.2E-159	mCD301b+ DTR
Ccl17	1.1178	0.792	0.637	4.2E-40	6.3E-36	mCD301b+ DTR
Pkib	1.0191	0.449	0.063	1.1E-93	1.7E-89	mCD301b+ DTR
Ramp3	0.9060	0.509	0.12	2.4E-82	3.6E-78	mCD301b+ DTR
Cst3	0.8259	0.999	0.999	6.0E-82	8.9E-78	mCD301b+ DTR
Gyg	0.8185	0.829	0.58	1.6E-68	2.4E-64	mCD301b+ DTR
Glipr2	0.8113	0.788	0.505	9.8E-84	1.5E-79	mCD301b+ DTR
AA467197	0.7371	0.486	0.212	7.1E-46	1.1E-41	mCD301b+ DTR
Txndc17	0.7205	0.947	0.816	1.7E-84	2.5E-80	mCD301b+ DTR
Cytip	0.7171	0.893	0.61	3.7E-90	5.6E-86	mCD301b+ DTR
Stat1	0.6552	0.706	0.367	1.3E-68	1.9E-64	mCD301b+ DTR
Bcl2l14	0.6154	0.421	0.137	1.9E-48	2.8E-44	mCD301b+ DTR
Ccl22	0.5922	0.922	0.778	2.6E-37	3.8E-33	mCD301b+ DTR
Slc27a3	0.5748	0.323	0.057	1.4E-55	2.1E-51	mCD301b+ DTR
Clta	0.5565	0.931	0.828	1.1E-73	1.6E-69	mCD301b+ DTR
Stat4	0.5362	0.391	0.095	1.3E-52	1.9E-48	mCD301b+ DTR
Serpinb6b	0.5220	0.923	0.781	4.4E-42	6.6E-38	mCD301b+ DTR
Got1	0.5161	0.443	0.177	8.2E-48	1.2E-43	mCD301b+ DTR

gene	avg_logFC	pct.1	pct.2	p_val	p_val_adj	cluster
Cd86	0.5121	0.523	0.269	2.4E-37	3.6E-33	mCD301b+ DTR
Pdcd1lg2	0.4999	0.367	0.084	3.9E-54	5.8E-50	mCD301b+ DTR
Rps27l	0.4585	0.977	0.959	7.8E-52	1.2E-47	mCD301b+ DTR
Syngr2	0.4536	0.976	0.896	7.0E-64	1.0E-59	mCD301b+ DTR
Plgrkt	0.4482	0.597	0.349	2.8E-37	4.2E-33	mCD301b+ DTR
Ccnd2	0.4410	0.215	0.056	4.9E-28	7.4E-24	mCD301b+ DTR
Tspo	0.4360	0.976	0.936	1.1E-44	1.7E-40	mCD301b+ DTR
Actg1	0.4239	1	0.989	2.2E-50	3.3E-46	mCD301b+ DTR
Cmc2	0.4229	0.407	0.185	2.6E-28	3.9E-24	mCD301b+ DTR
Ndrg1	0.4087	0.463	0.244	4.1E-25	6.2E-21	mCD301b+ DTR
Rab8b	0.4077	0.685	0.455	6.3E-32	9.5E-28	mCD301b+ DTR
Selm	0.4049	0.626	0.5	4.1E-13	6.1E-09	mCD301b+ DTR
Irf8	0.4034	0.765	0.648	6.7E-18	1.0E-13	mCD301b+ DTR
Lgals1	0.4004	0.658	0.579	5.1E-22	7.7E-18	mCD301b+ DTR
Lcp1	0.3991	0.737	0.542	1.0E-27	1.6E-23	mCD301b+ DTR
Gdi2	0.3987	0.856	0.668	2.5E-39	3.8E-35	mCD301b+ DTR
Cd80	0.3964	0.326	0.095	1.6E-35	2.4E-31	mCD301b+ DTR
Zfand6	0.3959	0.875	0.748	1.7E-37	2.5E-33	mCD301b+ DTR
Ncoa7	0.3844	0.421	0.209	8.1E-27	1.2E-22	mCD301b+ DTR
Lactb	0.3835	0.574	0.347	1.2E-29	1.8E-25	mCD301b+ DTR
Il7r	0.3805	0.453	0.248	1.2E-26	1.7E-22	mCD301b+ DTR
Ptpn1	0.3785	0.442	0.213	5.2E-29	7.8E-25	mCD301b+ DTR
Serpinb9	0.3770	0.846	0.712	6.6E-24	9.8E-20	mCD301b+ DTR
Crem	0.3695	0.255	0.059	1.0E-32	1.6E-28	mCD301b+ DTR
Pmvk	0.3618	0.615	0.412	3.4E-23	5.2E-19	mCD301b+ DTR
Calm1	0.3605	0.997	0.997	5.2E-35	7.8E-31	mCD301b+ DTR
Txn1	0.3591	0.943	0.878	1.8E-27	2.7E-23	mCD301b+ DTR
Amica1	0.3543	0.292	0.087	8.1E-31	1.2E-26	mCD301b+ DTR
Serpina3g	0.3438	0.33	0.13	4.4E-26	6.6E-22	mCD301b+ DTR
Rab14	0.3435	0.755	0.559	1.2E-27	1.8E-23	mCD301b+ DTR
Mif4gd	0.3379	0.524	0.299	2.4E-24	3.6E-20	mCD301b+ DTR
Tspan13	0.3313	0.615	0.426	4.3E-21	6.4E-17	mCD301b+ DTR
Adprh	0.3298	0.434	0.201	9.6E-28	1.4E-23	mCD301b+ DTR
Lyz2	0.3228	0.597	0.449	4.3E-10	6.4E-06	mCD301b+ DTR
S100a6	0.3193	0.952	0.896	3.7E-22	5.5E-18	mCD301b+ DTR
Nt5c	0.3176	0.647	0.435	2.1E-23	3.1E-19	mCD301b+ DTR
Capg	0.3176	0.628	0.432	1.4E-20	2.2E-16	mCD301b+ DTR
Slamf1	0.3162	0.333	0.152	7.2E-21	1.1E-16	mCD301b+ DTR
Cd302	0.3159	0.292	0.134	2.9E-20	4.4E-16	mCD301b+ DTR
Myl6	0.3157	0.986	0.981	2.6E-24	3.9E-20	mCD301b+ DTR
Rac1	0.3135	0.87	0.739	1.1E-26	1.6E-22	mCD301b+ DTR
Lrrfip1	0.3126	0.436	0.246	1.0E-20	1.5E-16	mCD301b+ DTR
Akap9	0.3125	0.486	0.296	1.9E-19	2.9E-15	mCD301b+ DTR
Tpm4	0.3093	0.767	0.612	3.4E-20	5.1E-16	mCD301b+ DTR
Cd274	0.3074	0.658	0.423	4.6E-24	6.8E-20	mCD301b+ DTR
Dnajc12	0.3058	0.345	0.145	8.5E-24	1.3E-19	mCD301b+ DTR
Fabp5	0.3056	0.958	0.937	1.8E-12	2.6E-08	mCD301b+ DTR
Mrpl13	0.3035	0.431	0.246	2.0E-19	3.0E-15	mCD301b+ DTR
Cd200	0.3032	0.418	0.24	4.8E-16	7.2E-12	mCD301b+ DTR
Ywhah	0.3011	0.77	0.603	2.9E-22	4.3E-18	mCD301b+ DTR
Coro1a	0.3005	0.656	0.497	1.7E-15	2.5E-11	mCD301b+ DTR

Supplemental Table 5 – related to Figure 4. DE between mCD301b$^-$ and mCD301b$^+$ in control and *Foxp3^{DTR}* tdLN

(**A**) DE was performed where mCD301b$^-$ or mCD301b$^+$ from *Foxp3^{DTR}* tdLN were compared. Relates to volcano plot in Supplemental Figure 4J. Supplementary Table 5B lists all DE genes with log *N* fold change > 0.4. DE parameters: min.pct = 0.25. (**B**) DE was performed where either mCD301b$^-$ or mCD301b$^+$ from control tdLN and *Foxp3^{DTR}* tdLN were compared. Volcano plot in Figure 4D displayed all DE genes but highlighted genes with log *N* fold change >0.4. Supplementary Table 5A lists all DE genes with log *N* fold change > 0.3. DE parameters: min.pct = 0.1.

Supplemental Table 6

gene	avg_logFC	pct.1	pct.2	p_val	p_val_adj	cluster
FCER1A	1.4134	0.839	0.243	6.7E-121	1.2E-116	0
CD1C	1.1697	0.766	0.2	1.2E-120	2.1E-116	0
CLEC10A	1.1260	0.917	0.546	5.5E-90	9.5E-86	0
CD1E	0.9994	0.64	0.177	4.0E-82	6.9E-78	0
LGALS2	0.8471	0.967	0.567	1.6E-85	2.7E-81	0
AREG	0.8340	0.937	0.788	2.8E-46	4.9E-42	0
CFP	0.8269	0.94	0.508	1.4E-94	2.5E-90	0
NDRG2	0.7004	0.829	0.297	2.9E-105	5.1E-101	0
JAML	0.6790	0.995	0.867	4.0E-93	6.9E-89	0
LTB	0.6416	0.748	0.494	4.8E-34	8.3E-30	0
CXCL10	1.5549	0.494	0.196	4.1E-36	7.2E-32	1
S100A8	1.3196	0.736	0.537	2.2E-26	3.9E-22	1
S100A9	1.0608	0.907	0.789	1.7E-26	2.9E-22	1
VAMP5	0.9384	0.902	0.655	1.7E-73	2.9E-69	1
TIMP1	0.9195	0.928	0.881	8.6E-27	1.5E-22	1
CXCL9	0.9069	0.39	0.16	9.1E-27	1.6E-22	1
GBP1	0.9015	0.783	0.471	1.1E-52	2.0E-48	1
FCN1	0.8446	0.744	0.479	1.8E-30	3.2E-26	1
VCAN	0.8344	0.486	0.277	2.2E-18	3.9E-14	1
STAT1	0.7899	0.879	0.577	1.4E-65	2.4E-61	1
CXCL2	0.5477	0.507	0.39	1.3E-08	2.3E-04	2
PHACTR1	0.5477	0.899	0.68	2.1E-42	3.6E-38	2
AREG	0.5328	0.896	0.802	1.0E-17	1.8E-13	2
LYZ	0.5173	1	0.986	1.6E-49	2.9E-45	2
THBD	0.5119	0.738	0.469	1.9E-32	3.4E-28	2
HES1	0.5019	0.447	0.206	5.1E-24	8.9E-20	2
RGS2	0.4688	0.992	0.932	7.3E-31	1.3E-26	2
ZNF331	0.4607	0.872	0.695	1.9E-25	3.3E-21	2
OSM	0.4513	0.523	0.359	4.1E-13	7.1E-09	2
HBEGF	0.4399	0.796	0.565	5.5E-25	9.6E-21	2
APOE	2.2950	0.996	0.61	4.2E-122	7.3E-118	3
RNASE1	1.9069	0.773	0.328	4.4E-64	7.7E-60	3
APOC1	1.8721	0.992	0.518	1.3E-113	2.3E-109	3
SEPP1	1.8631	0.909	0.326	3.5E-104	6.2E-100	3
IFI27	1.8423	0.657	0.185	9.7E-70	1.7E-65	3
C1QB	1.7300	1	0.782	1.3E-111	2.2E-107	3
FOLR2	1.6111	0.913	0.264	4.9E-123	8.5E-119	3
C1QA	1.5937	1	0.806	5.4E-109	9.4E-105	3
PLTP	1.5914	0.938	0.284	2.6E-129	4.6E-125	3
HAMP	1.5868	0.756	0.179	2.9E-96	5.1E-92	3
SPP1	2.3263	0.826	0.457	1.1E-41	2.0E-37	4
NUPR1	1.8168	0.584	0.168	4.7E-43	8.3E-39	4
GPNMB	1.4000	0.842	0.259	3.3E-63	5.7E-59	4
HSPB1	1.2162	0.853	0.651	7.8E-11	1.4E-06	4
HSPA1A	1.1509	0.705	0.463	5.5E-13	9.7E-09	4
PLIN2	1.0907	0.789	0.518	5.2E-18	9.1E-14	4
RNASE1	1.0631	0.9	0.328	5.9E-64	1.0E-59	4
LGALS1	0.9891	1	0.956	8.1E-32	1.4E-27	4
BNIP3	0.9039	0.505	0.144	1.1E-37	1.9E-33	4
CSTB	0.8899	0.989	0.946	8.3E-15	1.4E-10	4

CLEC9A	1.8351	0.941	0.03	4.8E-237	8.4E-233	5
IDO1	1.7890	0.971	0.192	4.7E-96	8.3E-92	5
CPNE3	1.6050	1	0.423	2.2E-70	3.9E-66	5
DNASE1L3	1.5903	0.951	0.328	4.3E-59	7.4E-55	5
SNX3	1.4938	1	0.919	3.8E-58	6.7E-54	5
HIST1H4C	1.4578	0.784	0.451	5.3E-14	9.2E-10	5
C1orf54	1.2818	0.98	0.524	4.5E-55	7.9E-51	5
S100B	1.2652	0.745	0.391	1.8E-21	3.1E-17	5
IRF8	1.2457	0.98	0.664	6.4E-52	1.1E-47	5
LGALS2	1.2163	0.98	0.639	1.3E-41	2.3E-37	5
CCR7	3.0469	0.96	0.05	5.0E-84	8.8E-80	6
BIRC3	2.7268	1	0.532	1.6E-19	2.8E-15	6
CCL19	2.6507	0.88	0.065	8.6E-58	1.5E-53	6
MARCKSL1	2.5294	1	0.515	1.2E-19	2.0E-15	6
FSCN1	2.4204	0.96	0.211	1.0E-28	1.8E-24	6
CRIP1	2.1336	1	0.592	4.6E-17	8.0E-13	6
EBI3	2.0899	0.8	0.176	1.5E-20	2.5E-16	6
TXN	1.9230	1	0.829	6.4E-16	1.1E-11	6
IDO1	1.8681	0.8	0.23	1.9E-15	3.4E-11	6
IL7R	1.6540	0.92	0.039	2.0E-90	3.5E-86	6

Supplemental Table 6 – related to Figure 6. Top 10 DE genes between all myeloid clusters in human tdLN scRNA-Seq

DE was performed where every cluster was compared to all remaining cells. The top 10 DE genes for each cluster was selected and displayed in the Figure 6B and Supplementary Table 6. DE parameters: logfc.threshold = 0.4, min.pct = 0.25.

Supplemental Figure 7

gene	avg_logFC	pct.1	pct.2	p_val	p_val_adj	cluster
DDIT4	0.3954	0.911	0.765	1.0E-09	1.8E-05	0.1
CORO1A	0.3129	1	0.978	2.3E-14	4.0E-10	0.1
LIMD2	0.2937	0.975	0.933	9.0E-11	1.6E-06	0.1
GYPC	0.2925	0.519	0.287	1.4E-07	2.4E-03	0.1
HINT1	0.2829	1	0.974	1.0E-11	1.8E-07	0.1
CRIP1	0.2788	0.924	0.81	8.2E-07	1.4E-02	0.1
ACTB	0.2742	1	1	3.7E-14	6.4E-10	0.1
PDLIM1	0.2706	0.424	0.142	5.3E-12	9.2E-08	0.1
SRSF2	0.2626	0.981	0.888	5.7E-09	9.9E-05	0.1
GSTP1	0.2543	1	0.993	8.2E-13	1.4E-08	0.1
SEPT6	0.2464	0.797	0.634	3.3E-07	5.8E-03	0.1
SRSF3	0.2443	0.994	0.929	1.3E-07	2.2E-03	0.1
ANXA6	0.2413	0.734	0.593	1.7E-06	2.9E-02	0.1
HNRNPK	0.2365	1	0.963	1.2E-08	2.0E-04	0.1
CXCR4	0.2345	1	0.974	1.5E-06	2.5E-02	0.1
COTL1	0.2301	1	0.996	4.9E-08	8.6E-04	0.1
ACTG1	0.2273	1	1	4.8E-10	8.3E-06	0.1
MYL12A	0.2230	1	0.996	5.5E-09	9.6E-05	0.1
HLA-DOB	0.2205	0.449	0.235	7.5E-07	1.3E-02	0.1
SNX3	0.2198	0.981	0.937	2.1E-06	3.7E-02	0.1
PRELID1	0.2186	1	0.963	2.0E-06	3.5E-02	0.1
CAP1	0.2132	0.994	0.948	1.0E-06	1.8E-02	0.1
RPSA	0.1942	1	1	1.5E-12	2.6E-08	0.1
SYTL1	0.1874	0.399	0.183	3.4E-07	6.0E-03	0.1
NPM1	0.1868	1	1	7.3E-07	1.3E-02	0.1
GDI2	0.1866	0.981	0.966	2.8E-07	4.9E-03	0.1
PFN1	0.1831	1	1	5.8E-10	1.0E-05	0.1
LSP1	0.1711	1	0.993	8.2E-07	1.4E-02	0.1
GAPDH	0.1674	1	1	4.5E-07	7.8E-03	0.1
RPL10A	0.1618	1	1	1.9E-12	3.2E-08	0.1
HNRNPA2B1	0.1564	1	0.985	1.3E-06	2.3E-02	0.1
RPL8	0.1562	1	1	5.1E-13	8.8E-09	0.1
RPL5	0.1560	1	1	7.9E-10	1.4E-05	0.1
RPS17	0.1513	1	1	3.1E-11	5.3E-07	0.1
C14orf2	0.1467	1	0.974	2.7E-06	4.6E-02	0.1
RPS5	0.1448	1	1	2.7E-10	4.7E-06	0.1
RPS23	0.1334	1	1	4.9E-10	8.5E-06	0.1
NACA	0.1310	1	1	2.8E-06	4.8E-02	0.1
RPS18	0.1261	1	1	1.8E-09	3.2E-05	0.1
RPS3	0.1243	1	1	3.5E-10	6.2E-06	0.1
RPS3A	0.1234	1	1	3.4E-09	5.9E-05	0.1
RPL9	0.1215	1	1	1.6E-07	2.7E-03	0.1
RPL18A	0.1208	1	1	7.0E-10	1.2E-05	0.1
RPL18	0.1186	1	1	5.7E-08	9.9E-04	0.1
RPS7	0.1179	1	1	3.7E-08	6.4E-04	0.1
RPS13	0.1173	1	1	1.6E-08	2.8E-04	0.1
RPL7A	0.1146	1	1	1.2E-06	2.2E-02	0.1
RPL19	0.1110	1	1	1.1E-07	1.9E-03	0.1
RPS2	0.1101	1	1	1.7E-06	2.9E-02	0.1
RPS6	0.1075	1	1	6.0E-08	1.0E-03	0.1

RPL13A	0.1048	1	1	1.1E-06	1.9E-02	0.1
RPS11	0.1041	1	1	2.2E-06	3.8E-02	0.1
RPS15	0.1004	1	1	5.7E-07	9.9E-03	0.1
DNASE1L3	1.5074	0.752	0.346	1.6E-22	2.8E-18	0.2
CCL4L2	1.2087	0.664	0.329	1.2E-14	2.2E-10	0.2
C1QA	1.0690	0.861	0.702	3.1E-16	5.4E-12	0.2
HLA-DQB2	1.0322	0.628	0.135	5.1E-27	9.0E-23	0.2
CD1E	0.9392	0.861	0.529	2.7E-21	4.7E-17	0.2
CCL3L3	0.9381	0.708	0.37	3.4E-13	6.0E-09	0.2
C1QB	0.8877	0.839	0.647	1.4E-12	2.4E-08	0.2
C1QC	0.8721	0.642	0.46	9.2E-08	1.6E-03	0.2
CCL4	0.7649	0.562	0.239	1.4E-11	2.4E-07	0.2
MT2A	0.6880	0.81	0.564	7.4E-10	1.3E-05	0.2
CCL3	0.6767	0.723	0.554	9.9E-07	1.7E-02	0.2
S100B	0.6617	0.562	0.27	9.4E-10	1.6E-05	0.2
CXCL8	0.6254	0.62	0.384	1.5E-06	2.5E-02	0.2
IDO1	0.6155	0.46	0.17	9.5E-11	1.7E-06	0.2
STAT1	0.5936	0.715	0.346	1.1E-16	1.9E-12	0.2
ACP5	0.5706	0.759	0.256	1.0E-24	1.8E-20	0.2
GBP1	0.5565	0.708	0.408	1.1E-11	1.8E-07	0.2
TMEM176B	0.5429	0.467	0.235	3.3E-08	5.8E-04	0.2
IFITM3	0.5387	0.978	0.772	4.2E-13	7.3E-09	0.2
CD1B	0.5358	0.423	0.128	1.5E-12	2.7E-08	0.2
FAM26F	0.5056	0.978	0.927	9.7E-17	1.7E-12	0.2
CD68	0.4581	0.927	0.779	2.7E-13	4.7E-09	0.2
PLA2G7	0.4254	0.635	0.356	3.8E-09	6.6E-05	0.2
TUBB	0.4107	0.876	0.772	4.2E-07	7.3E-03	0.2
LGALS2	0.4084	1	0.955	1.6E-13	2.9E-09	0.2
GSN	0.4023	0.993	0.979	4.8E-13	8.4E-09	0.2
HLA-DQA2	0.3966	0.277	0.035	6.5E-14	1.1E-09	0.2
CLEC10A	0.3903	0.978	0.896	1.8E-09	3.2E-05	0.2
EGR2	0.3857	0.409	0.125	2.8E-11	4.9E-07	0.2
SERPINF1	0.3671	0.759	0.433	7.2E-11	1.3E-06	0.2
RGS10	0.3538	0.985	0.948	2.6E-13	4.5E-09	0.2
PLEKHO1	0.3524	0.876	0.678	4.2E-08	7.3E-04	0.2
PTMS	0.3417	0.73	0.429	3.5E-10	6.1E-06	0.2
C1orf54	0.3397	0.526	0.26	5.6E-09	9.8E-05	0.2
NAP1L1	0.3375	1	0.99	2.0E-14	3.4E-10	0.2
HCAR2	0.3337	0.474	0.173	1.8E-10	3.1E-06	0.2
MMP9	0.3315	0.255	0.076	3.4E-07	5.9E-03	0.2
FTL	0.3141	1	1	1.6E-07	2.7E-03	0.2
HLA-DQB1	0.3001	1	1	9.7E-17	1.7E-12	0.2
NPC2	0.2953	0.993	0.983	2.6E-09	4.5E-05	0.2
HLA-DPB1	0.2845	1	1	2.3E-15	4.0E-11	0.2
ENPP2	0.2837	0.584	0.263	3.3E-10	5.8E-06	0.2
ITM2B	0.2813	1	1	1.3E-09	2.3E-05	0.2
FGL2	0.2746	0.985	0.99	1.1E-06	1.9E-02	0.2
SLAMF7	0.2738	0.555	0.263	8.7E-09	1.5E-04	0.2
HLA-DRB5	0.2732	1	1	1.0E-20	1.8E-16	0.2
SLAMF8	0.2723	0.701	0.405	2.9E-08	5.1E-04	0.2
CD63	0.2691	0.985	0.962	3.2E-07	5.6E-03	0.2
LGALS3BP	0.2657	0.474	0.173	5.1E-11	8.9E-07	0.2
NINJ1	0.2656	0.606	0.346	1.7E-06	2.9E-02	0.2

PNRC1	0.2606	0.964	0.952	5.3E-07	9.3E-03	0.2
PILRA	0.2601	0.788	0.564	3.4E-07	5.9E-03	0.2
TMEM176A	0.2544	0.372	0.135	2.2E-08	3.9E-04	0.2
GBP4	0.2505	0.613	0.367	1.6E-06	2.9E-02	0.2
FRMD4B	0.2484	0.613	0.325	6.7E-08	1.2E-03	0.2
HLA-DQA1	0.2368	1	1	4.6E-12	8.0E-08	0.2
HLA-DRA	0.2352	1	1	1.9E-20	3.3E-16	0.2
CST3	0.2165	1	1	2.2E-09	3.9E-05	0.2
PVRL2	0.2145	0.584	0.336	1.0E-06	1.8E-02	0.2
GPR34	0.2130	0.409	0.149	1.2E-08	2.1E-04	0.2
LPAR6	0.2120	0.489	0.225	3.4E-07	5.9E-03	0.2
HLA-DRB1	0.2115	1	1	7.9E-14	1.4E-09	0.2
HLA-DPA1	0.2097	1	1	2.6E-12	4.5E-08	0.2
HLA-E	0.2032	0.985	0.99	2.6E-06	4.5E-02	0.2
CD74	0.2006	1	1	7.8E-20	1.4E-15	0.2
CPVL	0.1980	1	0.993	2.3E-06	4.0E-02	0.2
TYROBP	0.1941	1	0.997	2.4E-06	4.3E-02	0.2
TPT1	0.1813	1	1	1.6E-11	2.9E-07	0.2
B2M	0.1775	1	1	5.2E-09	9.1E-05	0.2
IL6ST	0.1770	0.38	0.138	6.9E-08	1.2E-03	0.2
HLA-DMB	0.1709	0.993	1	1.5E-06	2.6E-02	0.2
SERPING1	0.1649	0.314	0.114	1.2E-06	2.2E-02	0.2
ELAVL4	0.1300	0.27	0.083	4.6E-07	7.9E-03	0.2
FCGR1B	0.1282	0.328	0.121	2.3E-06	4.0E-02	0.2
FCN1	1.1242	0.679	0.342	4.4E-18	7.7E-14	0.3
S100A9	1.0495	0.779	0.559	1.2E-14	2.0E-10	0.3
FCER1A	0.9011	0.924	0.803	2.5E-13	4.4E-09	0.3
S100A4	0.8120	0.992	0.915	3.7E-24	6.5E-20	0.3
S100A8	0.7891	0.489	0.298	5.1E-07	8.9E-03	0.3
CD14	0.6979	0.893	0.631	1.2E-17	2.1E-13	0.3
TSPO	0.6136	0.977	0.722	7.6E-23	1.3E-18	0.3
HBEGF	0.5721	0.763	0.492	3.4E-12	6.0E-08	0.3
VCAN	0.5464	0.412	0.071	2.5E-19	4.3E-15	0.3
S100A6	0.5026	1	0.98	2.0E-16	3.5E-12	0.3
FCGR2A	0.3600	0.679	0.529	1.2E-08	2.1E-04	0.3
SAMSN1	0.3526	0.779	0.603	2.3E-07	3.9E-03	0.3
RHOB	0.3499	0.595	0.414	2.1E-06	3.6E-02	0.3
ID3	0.3399	0.298	0.085	1.0E-08	1.8E-04	0.3
CAPG	0.3327	0.878	0.851	2.0E-07	3.4E-03	0.3
NUP214	0.3248	0.481	0.186	8.7E-12	1.5E-07	0.3
TGIF1	0.3215	0.656	0.481	2.7E-06	4.6E-02	0.3
NAMPT	0.3153	0.954	0.888	3.1E-08	5.4E-04	0.3
SERPINA1	0.3059	0.962	0.908	1.3E-08	2.3E-04	0.3
CD1D	0.3042	0.763	0.624	1.6E-07	2.7E-03	0.3
FCGRT	0.2945	0.992	0.973	5.8E-10	1.0E-05	0.3
NEAT1	0.2937	1	0.993	8.3E-09	1.4E-04	0.3
CTSS	0.2906	1	0.997	1.9E-10	3.3E-06	0.3
NPC2	0.2903	0.985	0.986	2.8E-09	4.8E-05	0.3
LY96	0.2894	0.779	0.634	2.5E-07	4.4E-03	0.3
HNMT	0.2870	0.55	0.305	5.1E-08	9.0E-04	0.3
TKT	0.2779	0.931	0.939	1.8E-06	3.1E-02	0.3
F13A1	0.2660	0.344	0.125	1.3E-08	2.2E-04	0.3
SLC11A1	0.2518	0.328	0.122	3.3E-08	5.7E-04	0.3

MT-ND3	0.2388	0.992	1	1.2E-07	2.2E-03	0.3
PSAP	0.2281	1	0.997	5.9E-07	1.0E-02	0.3
FCER1G	0.2226	1	0.997	3.8E-08	6.7E-04	0.3
LAPTM5	0.2193	0.992	0.993	1.2E-08	2.0E-04	0.3
MT-ND2	0.2174	1	0.997	2.0E-08	3.6E-04	0.3
SNCA	0.2147	0.336	0.105	1.2E-09	2.1E-05	0.3
CD2	0.2134	0.412	0.2	5.3E-07	9.2E-03	0.3
CD300E	0.2122	0.305	0.125	6.4E-07	1.1E-02	0.3
TYROBP	0.2107	1	0.997	5.8E-10	1.0E-05	0.3
S100A12	0.2042	0.252	0.054	2.1E-09	3.6E-05	0.3
AIF1	0.2010	0.992	1	1.7E-06	3.0E-02	0.3
FTL	0.1999	1	1	6.9E-10	1.2E-05	0.3
MT-CO3	0.1877	0.992	1	2.4E-06	4.1E-02	0.3
MT-ND1	0.1858	0.992	0.997	2.1E-06	3.6E-02	0.3
H3F3A	0.1427	1	1	6.1E-08	1.1E-03	0.3

Supplemental Table 7 – related to Figure 6. DE genes between BDCA-1^{+} cDC2 clusters 0.1 – 0.3

DE was performed where BDCA-1+ cDC2 clusters 0.1, 0.2 and 0.3 were compared to one another. All DE genes above the logFC threshold are displayed in Figure 6D as heatmap and in Supplementary Table 7. DE parameters: logfc.threshold = 0.1, min.pct = 0.25.

Materials and Methods

Human Tumor Samples

The human head and neck tumor set consisted of a total of 32 tumors removed from the head and neck region, agnostic to location. The anti-PD-1 responder/non-responder melanoma tumor set was published previously (Barry et al., 2018). All patients consented for tissue collection under a UCSF IRB approved protocol (UCSF IRB# 13-12246 and 14-15342). Samples were obtained after surgical excision with biopsies taken by the Pathology Department to confirm the presence of tumor cells. Patients were selected without regard to prior treatment. Freshly resected samples were placed in ice-cold PBS or Leibovitz's L-15 medium in a 50 mL conical tube and immediately transported to the laboratory for evaluation. Patient samples were coded and flow analysis was scored by separate individuals prior to data agglomeration. All samples were processed and analyzed by flow cytometry, but only those with at least 1,000 live $CD45^+$ cell events were included in the analysis.

Mice

All mice were treated in accordance with the regulatory standards of the National Institutes of Health and American Association of Laboratory Animal Care and were approved by the UCSF Institution of Animal Care and Use Committee. The following mice were purchased for acute use or maintained under specific pathogen-free conditions at the University of California, San Francisco Animal Barrier Facility. We attempted to use *Irf4*$^{flox/flox}$;*CD11c-Cre* but discovered independent breeding cages were producing germline *Irf4* globally deficient pups, complicating our findings (data not shown).

Method Details

Tumor cell lines, tumor cell injections and tumor growth experiments

B16-F10 (ATCC, CRL-6475) was purchased. B16-ChOVA ($B16^{ChOVA}$), a derivative of B16-F10, was created through transduction of B16-F10 with an mCherry-OVA (ChOVA) fusion construct identical to that used in previous studies in our lab

(Engelhardt et al., 2012; Roberts et al., 2016). $B78^{ChOVA}$, derived from the parental B78 subline of B16, was generated in our laboratory and described previously (Broz et al., 2014). B16-ZsGreen ($B16^{ZsGr}$) was previously generated in our laboratory as described (Headley et al., 2016). $B16^{GM\text{-}CSF}$ (GVAX) (Dranoff et al., 1993) were acquired from the laboratory of Dr. Lawrence Fong at UC San Francisco. Adherent cell lines were cultured at 37°C in 5% CO_2 in DMEM (Invitrogen), 10% FCS (Benchmark), Pen/Strep/Glut (Invitrogen).

For tumor cell injection, adherent tumor cells were lifted using 0.05% Trypsin-EDTA (Thermo Fisher Scientific) and washed 3X with DPBS (Thermo Fisher Scientific). $1.0x10^5$ – $2.5x10^5$ tumor cells were resuspended in DPBS and mixed 1:1 with Matrigel GFR (Corning) for a final injection volume of 50 μL. Mice anesthetized with isoflurane (Henry Schein) were shaved on their flank and injected subcutaneously either unilaterally or bilaterally depending on the experimental setup.

For tumor measurements, tumors were typically measured 3 times per week using electronic calipers. Tumor volume was calculated through the formula $V = 0.5(w^2 \times l)$. Mice were removed from the study and euthanized when tumors exceeded a volume of 1000 mm^3.

Single Cell RNA Sequencing (scRNA-Seq)

For mouse scRNA-seq, live $CD90.2^-$ $B220^-$ $Ly6G^-$ $NK1.1^-CD11b^+$ and/or $CD11c^+$ cells were sorted from inguinal and axillary LN with a BD FACSAria Fusion. For human scRNA-seq, live $CD3^-CD19/20^-CD56^-$ cells were sorted from a melanoma-draining LN on a BD FACSAria Fusion. After sorting, cells were pelleted and resuspended at $1x10^3$ cells/μl in 0.04%BSA/PBA and loaded onto the Chromium Controller (10X Genomics). Samples were processed for single-cell encapsulation and cDNA library generation using the Chromium Single Cell 3' v2 Reagent Kits (10X Genomics). The library was subsequently sequenced on an Illumina HiSeq 4000 (Illumina).

Single Cell Data Processing

Sequencing data was processed using 10X Genomics Cell Ranger V1.2 pipeline. The Cell Ranger subroutine *mkfastq* converted raw, Illumina bcl files to fastqs which were

then passed to Cell Ranger's *count,* which aligned all reads using the aligner STAR (Dobin et al., 2013) against UCSC mm10 or GRCh38 genomes for mouse and human cells, respectively. After filtering reads with redundant unique molecular identifiers (UMI), *count* generated a final gene-cellular barcode matrix. Both *mkfastq* and *count* were run with default parameters.

Cellular Identification and Clustering

For each sample, the gene - barcode matrix was passed to the R (v. 3.4.3) software package Seurat (Satija et al., 2015) (http://satijalab.org/seurat) (v2.3.0) for all downstream analyses. We then filtered on cells that expressed a minimum of 200 genes and required that all genes be expressed in at least 3 cells. We also removed cells that contained > 5% reads associated with cell cycle genes (Kowalczyk et al., 2015; Macosko et al., 2015). Count data was then log2 transformed and scaled using each cell's proportion of cell cycle genes as a nuisance factor (implemented in Seurat's *ScaleData* function) to correct for any remaining cell cycle effect in downstream clustering and differential expression analyses. For each sample, principal component (PC) analysis was performed on a set of highly variable genes defined by Seurat's *FindVariableGenes* function. Genes associated with the resulting PCs (chosen by visual inspection of scree plots) were then used for graph-based cluster identification and subsequent dimensionality reduction using t-distributed stochastic neighbor embedding (tSNE). Cluster-based marker identification and differential expression were performed using Seurat's *FindAllMarkers* for all between-cluster comparisons.

ImmGen Signature Generation

To generate *a priori* signatures for the myeloid cell types that we expected to find in the mouse tdLN sample, we downloaded microarray based transcriptional profiles from the Immunological Genome Project data Phase 1(Heng and Painter, 2008) (GSE15907). See **Supplementary Table 1** for the specific samples used.

For each ImmGen population, we performed DE analysis comparing samples from the population of interest to the aggregate of the remaining 6 groups using the R package *limma* (Ritchie et al., 2015). We ordered the top 20 genes with the smallest

FDR values (Benjamini and Hochberg, 1995) by fold change (excluding any genes that were downregulated in the group of interest) and then cross referenced the resulting list with the single cell expression matrix from each sample. This left genes that were both highly differentially expressed in the IMMGEN profiles and expressed in our single cell data sets of interest. The top 10 genes (or fewer if less than 10 genes remained) by fold change were then median normalized and aggregated to create a single "signature gene" for each cell type. These signature genes were 0-1 scaled and plotted in the context of the *t*-SNE dimensionality reduction to show cellular location.

Sequencing Sample Aggregation

In order to generate pairwise aggregations between samples and control for potential batch effects, we used Seurat's Canonical Correlation Analysis (CCA) functionality. All post-filtered cells from each of the single sample analyses were used in the aggregate. CCA was performed on the union of the 2000 genes with highest dispersions from each dataset. The number of canonical correlation vectors (CCVs) used in downstream clustering and *t*-SNE analyses was chosen by visual inspection of heatmaps of genes associated with those top CCVs. Results were robust to moderate changes in this final number of CCVs.

Mouse Tissue Digestion and Flow Staining

Tumor and LN tissues were harvested and enzymatically digested with 0.2 mg/ml DNAse I (Sigma-Aldrich), 100 U/ml Collagenase I (Worthington Biochemical), and 500 U/ml Collagenase Type IV (Worthington Biochemical) for 30-45 minutes at 37 °C. TdLN included inguinal and axillary LN. Tumor samples were subjected to consistent agitation during this time and LN samples were rapidly pipetted at the half-point time. Samples were filtered to generate a single-cell suspension and washed with stain media (PBS, 2% FCS). For bone marrow cells, mouse femurs and tibias were flushed with stain media and subsequently underwent red blood cell lysis.

Cells harvested from these tissues or *in vitro* culture were washed with PBS and stained with Zombie NIR fixable viability dye (BioLegend) for 30 minutes at 4°C to distinguish live and dead cells. Cells were then washed with stain media and non-

specific binding was blocked with anti-CD16/32 (BioXCell), and 2% rat serum (Invitrogen) and 2% Armenian hamster serum (Innovative Research). Cell surface proteins were then stained on ice for 30 minutes. Cells were washed again and re-suspended with stain media prior to collection and analysis on a BD Fortesssa or LSR-II flow cytometer. When applicable, black latex beads were added to the sample for quantification of absolute cell number. For intracellular stains, cells were fixed and permeabilized with the FoxP3/Transcription Factor Staining Buffer Set (Thermo Fisher Scientific) after surface marker staining. Intracellular antibodies were stained in permeabilization buffer with 2% rat serum for at least 30 minutes at room temperature.

Human Tissue Digestion and Flow Staining

Tumor or LN tissue was thoroughly chopped with surgical scissors and transferred to GentleMACs C Tubes (Miltenyi Biotec) containing 20 uL/mL Liberase TL (5 mg/ml, Roche) and 50 U/ml DNAse I (Roche) in RPMI 1640 per 0.3 g tissue. GentleMACs C Tubes were then installed onto the GentleMACs Octo Dissociator (Miltenyi Biotec) and incubated according to the manufacturer's instructions. Samples were then quenched with 10 mL of sort buffer (PBS/2% FCS/2mM EDTA), filtered through 100 um filters and spun down. Red blood cell lysis was performed with 175 mM ammonium chloride.

Cells were then incubated with Human FcX (Biolegend) to prevent non-specific antibody binding. Cells were then washed in DPBS and incubated with Zombie Aqua Fixable Viability Dye (Biolegend). Following viability dye, cells were washed with sort buffer and incubated with cell surface antibodies for 30 minutes on ice and subsequently fixed in either Fixation Buffer (BD Biosciences) or in Foxp3/Transcription Factor Staining Buffer Set (ThermoFisher Scientific) if intracellular staining was required.

APC-T cell *In Vitro* Co-Culture Assays

APC populations were double-sorted (yield followed by purity) from tdLN using a BD FACSAria Fusion and co-cultured with $2x10^4$ isolated eFluor670-labeled OT-II T cells at a 1:5 ratio in complete RPMI (Pen/Strep, NEAA, NaPyr, 2-ME, 10% FCS) in 96-well V-

bottom plates. Cells were harvested for analysis 3 days later. OVA peptide 323-339 (GenScript) was added to wells at 1 μg/ml as a positive control.

Mouse T cell Isolation and *In Vivo* Adoptive T Cell Transfer

Inguinal, axillary, brachial, superficial cervical and mesenteric LN were isolated from CD45.1$^+$ OT-II mice. LN were smashed through 100 um filters and subsequently spun down and counted. CD4$^+$ T cells were then isolated using EasySep CD4 negative-selection kits (STEMCELL Technologies).

1x10^5 isolated CD45.1$^+$ CD4$^+$ OT-II T cells were either transferred immediately in cases of PMA/Ionomycin restimulation experiments or labeled with Cell Proliferation Dye eFluor670 (Thermo Fisher Scientific) and 1.0-5.0x10^5 cells were adoptively transferred to CD45.2$^+$ mice. LN were harvested for proliferation analysis at day 3 post-transfer and for PMA/ionomycin re-stimulation at day 7 post-transfer. *XCR1^{DTR}* and *Cx3cr1^{iDTR}* mice were treated with 500 ng of DT every other day beginning the day prior to OT-II transfer through the experimental end point. *Foxp3^{DTR}* mice were injected with DT for two days prior to OT-II transfer and then the day following OT-II transfer.

T Cell Cytokine Analysis

For cytokine analysis of endogenous or adoptively transferred T cells, cells from either LN or tumors were used for re-stimulation. Single cell suspensions were incubated with 50 ng/ml PMA (Sigma-Aldrich), 500 ng/ml ionomycin (Thermo Fisher Scientific), 3 μg/ml brefeldin A (Cayman Chemical Company), and 2μM monensin (Thermo Fisher Scientific) for 5-6 hours in complete RPMI and stained for surface and intracellular proteins using the Foxp3/Transcription Factor Staining Buffer Set (ThermoFisher Scientific).

In Vivo Treatments

For diphtheria toxin (DT), while treatment schedules varied depending upon mouse genetic strain or type of experiment, mice received 500 ng boluses of un-nicked DT (List Biologics, 150) intraperitoneally. *Foxp3^{DTR}, XCR1^{DTR}* and *Cx3cr1^{iDTR}* mice were typically injected on days 9, 10 and 12 followed by flow cytometric analysis at day 14.

For comparisons of $CD4^+$ T_{conv} priming between steady-state, tumor-bearing and influenza-infected conditions, mice were injected subcutaneously with either 20 μg of endotoxin-free ovalbumin (Invivogen) in 50 μl of PBS or $2.0x10^5$ B16ChOVA. Mice receiving influenza were infected intranasally with $1x10^5$ PFU of X31-OT-II (Thomas et al., 2006), prepared as previously described (GeurtsvanKessel et al., 2008).$CD45.1^+$ $OT\text{-}II^+$ $CD4^+$ T cells were transferred intravenously 2 days after ovalbumin and X31-OT-II treatment and 14 days after $B16^{ChOVA}$ injection.

To assess CD4/CD8 T cell dependency for tumor rejection following T_{reg} depletion or GVAX/anti-CTLA-4 treatment, mice were injected with 250 μg of isotype (Clone: LTF-2, BioXCell), anti-CD4 (Clone: GK1.5, BioXCell) or anti-CD8a (Clone: 2.43, BioXCell) was injected at days 10, 13 and 16 post-tumor injection for *Foxp3*^{DTR} and days 4, 7 and 10 for GVAX/anti-CTLA-4 treatment.

To assess the requirement of T cell LN egress, control or *Foxp3*^{DTR} mice were treated with 500 ng of DT on days 9, 10 and 12 post-tumor injection and with 200 μg FTY720 (Cayman Chemicals) every day beginning on day 8 post-tumor injection through the end of the experiment.

For Fc-modified anti-CTLA-4 experiments, mice were injected with $2x10^5$ $B16^{ZsGreen}$ cells. On days 7, 9, 10, 11 and 13 post-tumor injection, mice received 250 μg of mouse IgG2c isotype, anti-CTLA-4 IgG2c (modified clone 9D9, Bristol-Myers-Squibb), mouse IgG1 isotype or anti-CTLA-4 IgG1 (modified clone 9D9, Bristol-Myers-Squibb).

For GVAX/anti-CTLA-4 experiments, mice were injected with either $1x10^5$ (tumor growth) or $2x10^5$ B16-F10 (cellular analysis). On days 3, 6 and 9 post-tumor injection, mice were injected subcutaneously on their contralateral flank with either PBS or $1x10^6$ 50 Gy-irradiated GVAX cells and received either 250 μg anti-CTLA-4 (9H10, BioXCell) or Syrian hamster IgG isotype (BioXcell) on day 3, and 100 μg of antibody on days 6 and 9.

Statistical analysis and experimental design

Unless specifically noted, data displayed is from a representative experiment of ≥ 2 independent experiments. Experimental group assignment was determined by genotype

or, if all wild-type mice, by random designation. Error bars represent mean ± S.E.M. calculated using Prism unless otherwise noted. Statistical analyses were performed using GraphPad Prism software. For pairwise comparisons, unpaired T tests were used unless otherwise noted. For statistical measures between more than two groups, one-way ANOVA would be performed unless otherwise noted. Comparisons found to be nonsignificant are not shown. Investigators were not blinded to group assignment during experimental procedures or analysis.

Data and Software Availability

Data Resources

The accession number for the expression matrix for the single-cell RNA-sequencing reported in this paper is GEO: XXXXXXXXX

KEY RESOURCES TABLE

REAGENT or RESOURCE	SOURCE	IDENTIFIER
Antibodies		
anti-mouse CD11c BV650 (clone N418)	Biolegend	117339
anti-mouse/human CD11b BV605 (clone M1/70)	Biolegend	101257
anti-mouse CD103 BV421 (clone 2E7)	Biolegend	121421
anti-mouse Ly-6C BV711 (clone HK1.4)	Biolegend	128037
anti-mouse CD90.2 BV785 (clone 30-H12)	Biolegend	105331
anti-mouse/human CD45R/B220 BV785 (clone RA3-6B2)	Biolegend	103246
anti-mouse Ly-6G BV785 (clone IA8)	Biolegend	127645
anti-mouse Siglec F BV786 (clone E50-2440)	BD Biosciences	740956
anti-mouse NK1.1 BV785 (clone PK136)	Biolegend	108749
anti-mouse CD24 PE/Cy7 (clone M1/69)	Biolegend	101822
anti-mouse MHC-II AF700 (clone M5/114.15.2)	Biolegend	107622
anti-mouse CD301b PE or APC (clone URA-1)	Biolegend	146814, 146803
anti-mouse CD8a PerCP/Cy5.5 or PE/Cy7 (clone 53-6.7)	Biolegend	100734, 100722
anti-mouse F4/80 FITC (clone BM8)	Biolegend	123107
anti-mouse CD45 PerCP/Cy5.5 (clone A20)	Biolegend	110727
anti-mouse CD197/CCR7 PE	Biolegend	120105
anti-mouse CD9 AF647 (clone MZ3)	Biolegend	124809
anti-mouse CD135/FLT3 PE (clone A2F10)	Biolegend	135305
anti-mouse CD172a/SIRPA PE or AF488 (clone P84)	Biolegend	144011,144023
anti-mouse CD14 PE (clone Sa14-2)	Biolegend	123309
anti-mouse CD16/32 PE (clone 93)	Biolegend	101307
anti-mouse CD200R PE (clone OX110)	Biolegend	123907
anti-mouse CD206 PE (clone C068C2)	Biolegend	141705
anti-mouse B7-H1 PE (PD-L1/CD274) (clone 10F.9G2)	Biolegend	124307
anti-mouse B7-H2 PE (ICOS-L/CD275) (clone HK5.3)	Biolegend	107405
anti-mouse B7-H3 PE (CD276) (clone RTAA15)	Biolegend	123507
anti-mouse B7-DC (PD-L2/CD273) PE (clone TY25)	Biolegend	107205
anti-mouse CD85K (LILRB4) PE	Biolegend	144903
anti-mouse CD4 BUV395 (clone GK1.5)	BD Biosciences	563790
anti-mouse/rat/human CD278/ICOS APC (clone C398.4A)	Biolegend	313510
anti-mouse CD279/PD-1 PE (clone RMP1-14)	Biolegend	114118
anti-mouse/human CD44 BV711 (clone IM7)	Biolegend	103057
anti-mouse CD69 BV650 (clone H1.2F3)	Biolegend	104541
anti-mouse Foxp3 eF450 (clone FJK-16s)	Thermo Fisher	48-5773-82
anti-mouse/rat/human Foxp3 AF647 (clone 150D)	Biolegend	320014
anti-mouse IL-4 PE (clone 11B11)	Biolegend	504104
anti-mouse IL-17a BV421 (clone TC11-18H10.1)	Biolegend	506926
anti-mouse IFNg PE/Cy7 (clone XMG1.2)	Biolegend	505825
anti-mouse/human T-bet BV605 (clone 4B10)	Biolegend	644817
anti-mouse CD117 APC (clone 2B8)	Biolegend	105811
anti-mouse CD115 PerCP/Cy5.5 (clone AFS98)	Biolegend	135525
anti-mouse Ly6-G (clone IA8)	Biolegend	127603
anti-mouse CD3e (clone 145-2C11)	Biolegend	100303

anti-mouse CD127 (clone A7R34)	Biolegend	135005
anti-mouse NK1.1 (clone PK136)	Biolegend	108703
anti-mouse/human CD45R (RA3-6B2)	Biolegend	103203
anti-mouse TER-119 (clone TER-119)	Biolegend	116203
anti-mouse TCR γ/δ (clone GL3)	Biolegend	118103
Streptavidin BV421	Biolegend	405226
anti-human CD45 APC/e780 (clone HI30)	Thermo Fisher	47-0459-42
anti-human CD3e PerCP/e710 (clone OKT3)	Thermo Fisher	46-0037-42
anti-human HLA-DR BUV395 (clone G46-6)	BD Biosciences	564040
anti-human CD56 BUV737 (clone NCAM16.2)	BD Biosciences	564448
anti-human CD4 PE/Dazzle 594 (clone S3.5)	Biolegend	100455
anti-human CD8a BV605 (clone RPA-T8)	Biolegend	301039
anti-human CD127 BV650 (clone HIL-7R-M21)	BD Biosciences	563225
anti-human CD38 AF700 (clone HIT2)	Biolegend	303523
anti-human CD25 APC (clone 2A3)	BD Biosciences	340939
anti-human CD45RO PE (clone UCHL1)	BD Biosciences	561889
anti-human PD-1 BV786 (clone EH12)	BD Biosciences	563789
anti-human ICOS BV711 (clone DX29)	BD Biosciences	563833
anti-human FoxP3 PE/Cy7 (clone 236A/E7)	Thermo Fisher	25-4777-41
anti-human CTLA-4 BV421 (clone BNI3)	BD Biosciences	565931
anti-human/mouse/rat Ki67 AF488 (clone SolA15)	Thermo Fisher	11-5698-82
anti-human CD19 PerCP/e710 (clone H1B19)	Thermo Fisher	45-0199-42
anti-human CD20 PerCP/e710 (clone 2H7)	Thermo Fisher	45-0209-42
anti-human CD56 PerCP/e710 (clone CMSSB)	Thermo Fisher	46-0567-42
anti-human CD64 BUV737 (clone 10.1)	BD Biosciences	564425
anti-human CD11c AF700 (clone 3.9)	Thermo Fisher	56-0116-42
anti-human CD16 BV605 (clone 3G8)	Biolegend	302039
anti-human CD273/PDL2 BV650 (clone MIH18)	BD Biosciences	563844
anti-human/mouse TREM2 APC (clone 237920)	R&D Systems	FAB17291A
anti-human CD304 PE (clone 12C2)	Biolegend	354503
anti-human CD1C/BDCA-1 PE/Cy7 (clone L161)	Biolegend	331515
anti-human CD197 BV421 (clone G043H7)	Biolegend	353207
anti-human BDCA-3 FITC (clone AD5-14H12)	Miltenyi	130-098-843
anti-human PDL1 BV786 (clone MIH1)	BD Biosciences	563739
anti-human CD14 BV711 (clone M5E2)	Biolegend	301837
PE Rat IgG2a, k Isotype Ctrl Antibody (clone RTK2758)	Biolegend	400508
PE Rat IgG1, k Isotype Ctrl Antibody (clone RTK2071)	Biolegend	400408
APC Armenian Hamster IgG Isotype Ctrl Antibody (clone HTK888)	Biolegend	400912
BV605 Mouse IgG1, k Isotype Ctrl Antibody (clone MOPC-21)	Biolegend	400162
BV421 Mouse IgG2a, k Isotype Ctrl Antibody (clone MOPC-173)	Biolegend	400259
anti-mouse CD4 InVivoMab (clone GK1.5)	BioXCell	BE0003-1
anti-mouse CD8 InVivoMab (clone 2.43)	BioXCell	BE0061
anti-mouse CTLA-4 (CD152) InVivoMab (clone 9H10)	BioXCell	BE0131
Rat IgG2b, k InVivoMab	BioXCell	BE0090
Polyclonal Syrian hamster IgG InVivoMab	BioXCell	BE0087
anti-mouse CD16/32 InVivoMab	BioXCell	BE0307

anti-mouse CTLA-4 mouse IgG2c (modified clone 9D9)	Bristol-Myers-Squibb	
anti-mouse CTLA-4 mouse IgG1 (modified clone 9D9)	Bristol-Myers-Squibb	
mouse IgG2c isotype	Bristol-Myers-Squibb	
mouse IgG1 isotype	Bristol-Myers-Squibb	
Normal Rat Serum	Thermo Fisher	10710C
Armenian Hamster Serum	Innovative Research	IGHMA-SER
Biological Samples		
Human tumor samples	UC San Francisco	IRB # 13-12246 and 14-15342
Mouse tissue samples (LN, tumor)	UC San Francisco	IACUC: AN170208
Chemicals, Peptides, and Recombinant Proteins		
Matrigel GFR, Phenol-red free	Corning	356231
Collagenase, Type I	Worthington Biochemical	LS004197
Collagenase, Type IV	Worthington Biochemical	LS004189
DNAse I	Roche	10104159001
Liberase TL	Roche	5401020001
Human TruStain FcX	Biolegend	422302
Zombie Aqua Fixable Viability Kit	Biolegend	423102
Zombie NIR Fixable Viability Kit	Biolegend	423106
Brilliant Stain Buffer Plus	BD Biosciences	566385
Brefeldin A (BFA)	Sigma-Aldrich	B7651
Phorbol 12-myristate 13-acetate (PMA)	Sigma-Aldrich	P8139
Ionomycin	Invitrogen	I24222
Monensin Solution (1000X)	Thermo Fisher	00-4505-51
Diphtheria Toxin (unnicked)	List Biological Laboratories	150
FTY720	Cayman Chemical Company	10006292
eBioscience™ Cell Proliferation Dye eFluor™ 670		65-0840-85
Ovalbumin Endofit	Invivogen	Vac-pova
OVA peptide (323-339)	Genscript	RP10610-1
Critical Commercial Assays		
Chromium Single Cell 3' Library & Gel Bead Kit V2	10X Genomics	120237
BD Cytofix	BD Biosciences	554655
Foxp3/Transcription factor staining buffer set	Thermo Fisher	00-5523-00
EasySep Mouse $CD4^+$ T Cell Isolation kit	STEMCELL Technologies	19852
Deposited Data		
GEO XXXXXX		
Experimental Models: Cell Lines		
B16-F10	ATCC	CRL-6475
B16-ChOVA	UC San Francisco	N/A

B78-ChOVA	UC San Francisco	N/A
B16-GM-CSF	UC San Francisco	N/A
B16-ZsGreen	UC San Francisco	N/A
Experimental Models: Organisms/Strains		
Mouse: C57BL/6J	The Jackson Laboratory	000664
Mouse: B6 CD45.1 (B6.SJL-Ptprc^{a} Pepc^{b}/BoyJ)	The Jackson Laboratory	002014
Mouse: OT-II (B6.Cg-Tg(TcraTcrb)425Cbn/J	The Jackson Laboratory	004194
Mouse: *Irf4 fl/fl (*B6.129S1-*Irf4tm1Rdf*/J)	The Jackson Laboratory	009380
Mouse: *ActB-Cre* (FVB/N-*Tmem163*$^{Tg(ACTB-cre)2Mrt}$/J) received backcrossed to C57/Bl6	The Jackson Laboratory	003376
Mouse: *CD11c-Cre* (B6.Cg-Tg(Itgax-cre)1-1Reiz/J)	The Jackson Laboratory	008068
Mouse: *Cx3cr1*^{iDTR} (B6N.129P2-*Cx3cr1*$^{tm3(DTR)Litt}$/J)	The Jackson Laboratory	025629
Mouse: *Ccr7-/-* (B6.129P2(C)-*Ccr7*^{tm1Rfor}/J)	The Jackson Laboratory	006621
Mouse: *Zbtb46*^{GFP} *(*B6.129S6(C)-*Zbtb46*$^{tm1.1Kmm}$/J)	The Jackson Laboratory	027618
Mouse: *Foxp3*^{DTR} *(*B6.129(Cg)-*Foxp3*$^{tm3(DTR/GFP)Ayr}$/J)	The Jackson Laboratory	016958
Mouse: *Xcr1*^{DTR} *(*Xcr1$^{tm2(HBEGF/Venus)Ksho}$)	Tsuneyasu Kaisho, Osaka University	MGI: 5544058
Mouse: *Foxp3*$^{Cre/YFP}$ (B6.129(Cg)-*Foxp3*$^{tm4(YFP/icre)Ayr}$/J)	The Jackson Laboratory	016959
Mouse: *Itgb8*$^{fl/fl}$ (Itgb8^{tm2Lfr})	Michael Rosenblum, UC San Francisco	MGI: 3608910
Mouse: *Il-10*$^{fl/fl}$ (Il-10 flox)	Susan Kaech, Salk Institute. Generated by Werner Müller.	PMID: 15534372
Mouse: *Areg-/- (*Areg^{tm1Dle})	Marco Conti, UC San Francisco. Generated by David C. Lee.	MGI: 2176531
Software and Algorithms		
CellRanger 2.0	10X Genomics	10xgenomics.com
STAR	Dobin et.al. 2013	code.google.com/p/rna-star/.
Seurat	Satija et al. 2015	satijalab.org/seurat/
R: The Project for Statistical Computing		r-project.org

Supplemental References

Barry, K.C., Hsu, J., Broz, M.L., Cueto, F.J., Binnewies, M., Combes, A.J., Nelson, A.E., Loo, K., Kumar, R., Rosenblum, M.D.*, et al.* (2018). A natural killer–dendritic cell axis defines checkpoint therapy–responsive tumor microenvironments. Nature medicine.

Benjamini, Y., and Hochberg, Y. (1995). Controlling the False Discovery Rate: A Practical and Powerful Approach to Multiple Testing. Journal of the Royal Statistical Society Series B (Methodological) *57*, 289-300.

Broz, M.L., Binnewies, M., Boldajipour, B., Nelson, A.E., Pollack, J.L., Erle, D.J., Barczak, A., Rosenblum, M.D., Daud, A., Barber, D.L.*, et al.* (2014). Dissecting the tumor myeloid compartment reveals rare activating antigen-presenting cells critical for T cell immunity. Cancer Cell *26*, 638-652.

Dobin, A., Davis, C.A., Schlesinger, F., Drenkow, J., Zaleski, C., Jha, S., Batut, P., Chaisson, M., and Gingeras, T.R. (2013). STAR: ultrafast universal RNA-seq aligner. Bioinformatics (Oxford, England) *29*, 15-21.

Dranoff, G., Jaffee, E., Lazenby, A., Golumbek, P., Levitsky, H., Brose, K., Jackson, V., Hamada, H., Pardoll, D., and Mulligan, R.C. (1993). Vaccination with irradiated tumor cells engineered to secrete murine granulocyte-macrophage colony-stimulating factor stimulates potent, specific, and long-lasting anti-tumor immunity. Proceedings of the National Academy of Sciences of the United States of America *90*, 3539-3543.

Engelhardt, J.J., Boldajipour, B., Beemiller, P., Pandurangi, P., Sorensen, C., Werb, Z., Egeblad, M., and Krummel, M.F. (2012). Marginating dendritic cells of the tumor

microenvironment cross-present tumor antigens and stably engage tumor-specific T cells. Cancer Cell *21*, 402-417.

GeurtsvanKessel, C.H., Willart, M.A., van Rijt, L.S., Muskens, F., Kool, M., Baas, C., Thielemans, K., Bennett, C., Clausen, B.E., Hoogsteden, H.C.*, et al.* (2008). Clearance of influenza virus from the lung depends on migratory langerin+CD11b- but not plasmacytoid dendritic cells. The Journal of experimental medicine *205*, 1621-1634.

Headley, M.B., Bins, A., Nip, A., Roberts, E.W., Looney, M.R., Gerard, A., and Krummel, M.F. (2016). Visualization of immediate immune responses to pioneer metastatic cells in the lung. Nature *531*, 513-517.

Heng, T.S., and Painter, M.W. (2008). The Immunological Genome Project: networks of gene expression in immune cells. Nat Immunol *9*, 1091-1094.

Kowalczyk, M.S., Tirosh, I., Heckl, D., Rao, T.N., Dixit, A., Haas, B.J., Schneider, R.K., Wagers, A.J., Ebert, B.L., and Regev, A. (2015). Single-cell RNA-seq reveals changes in cell cycle and differentiation programs upon aging of hematopoietic stem cells. Genome research *25*, 1860-1872.

Macosko, E.Z., Basu, A., Satija, R., Nemesh, J., Shekhar, K., Goldman, M., Tirosh, I., Bialas, A.R., Kamitaki, N., Martersteck, E.M.*, et al.* (2015). Highly Parallel Genome-wide Expression Profiling of Individual Cells Using Nanoliter Droplets. Cell *161*, 1202-1214.

Ritchie, M.E., Phipson, B., Wu, D., Hu, Y., Law, C.W., Shi, W., and Smyth, G.K. (2015). limma powers differential expression analyses for RNA-sequencing and microarray studies. Nucleic acids research *43*, e47.

Roberts, Edward W., Broz, Miranda L., Binnewies, M., Headley, Mark B., Nelson, Amanda E., Wolf, Denise M., Kaisho, T., Bogunovic, D., Bhardwaj, N., and Krummel, Matthew F. (2016). Critical Role for CD103+/CD141+ Dendritic Cells Bearing CCR7 for Tumor Antigen Trafficking and Priming of T Cell Immunity in Melanoma. Cancer Cell *30*, 324-336.

Satija, R., Farrell, J.A., Gennert, D., Schier, A.F., and Regev, A. (2015). Spatial reconstruction of single-cell gene expression data. Nature biotechnology *33*, 495-502.

Thomas, P.G., Brown, S.A., Yue, W., So, J., Webby, R.J., and Doherty, P.C. (2006). An unexpected antibody response to an engineered influenza virus modifies CD8+ T cell responses. Proceedings of the National Academy of Sciences of the United States of America *103*, 2764-2769.